Electronic Supplementary Material (ESI) for New Journal of Chemistry.

Design, synthesis, anti-proliferative evaluation and docking studies of 1*H*-1,2,3-triazole tethered Ospemifene-isatin conjugates as Selective Estrogen Receptor Modulators

Sumit Kumar[a], Liang Gu[b], Gabriella Palma[b], MandeepKaur*[b], Ashona Singh-Pillay[c], Parvesh Singh*[c] and Vipan Kumar*[a]

[a]Department of Chemistry, Guru Nanak Dev University, Amritsar-143005, India
[b]School of Molecular and Cell Biology, University of the Witwatersrand, Private Bag 3, Wits-2050, Johannesburg, South Africa
[c] School of Chemistry and Physics, University of KwaZulu Natal, P/Bag X54001, Westville, Durban 4000, South Africa

^{1}H NMR of (Z)-(4-chloro-1-(4-(2-(prop2-yn-1-yloxy)ethoxy)phenyl)but-1-ene-1,2-diyl)dibenzene (4):

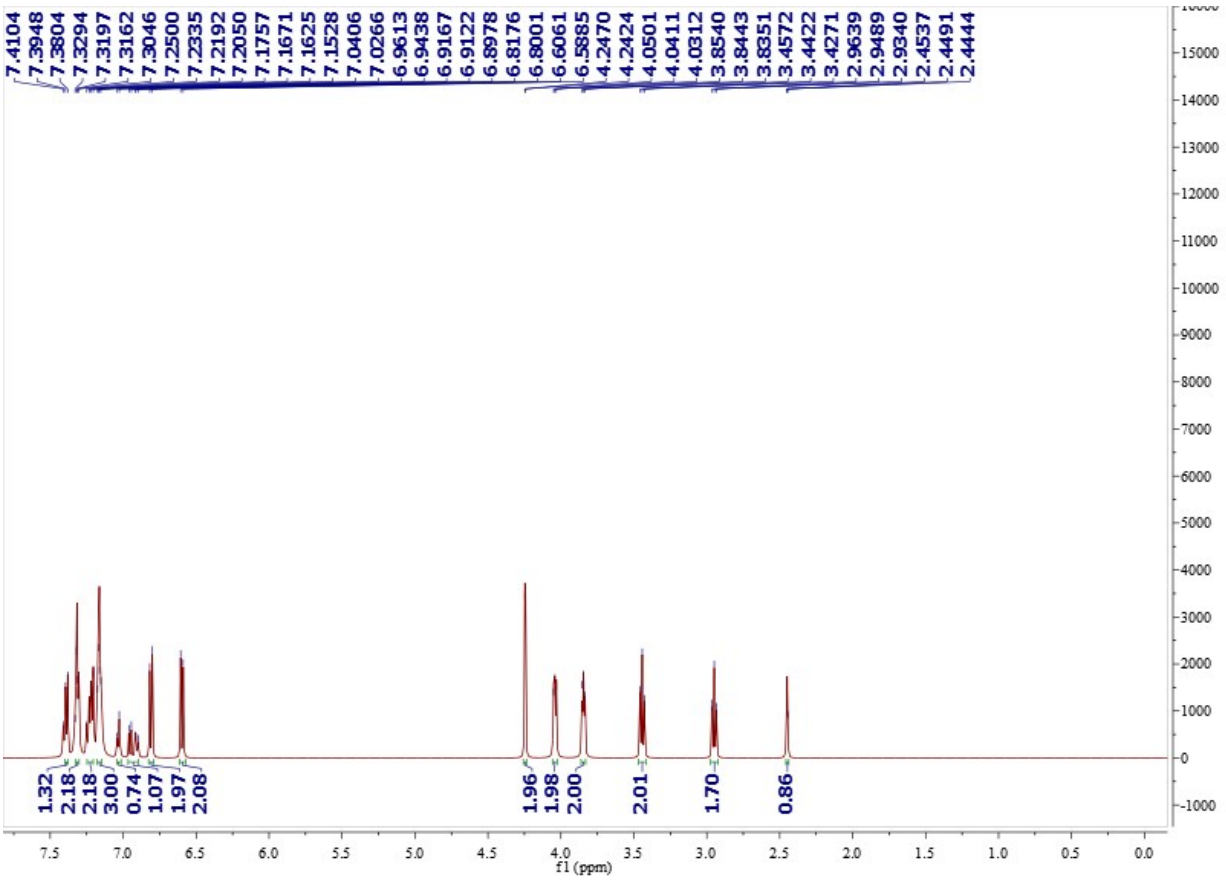

^{1}H NMR of (Z)-1-(5-(4-((2-(4(4-choro-1,2-diphenylbut-1-en-1yl)phenoxy)ethoxy)methyl)-1H-1,2,3-triazol-1-yl)pentyl)indoline-2,3-dione (11c):

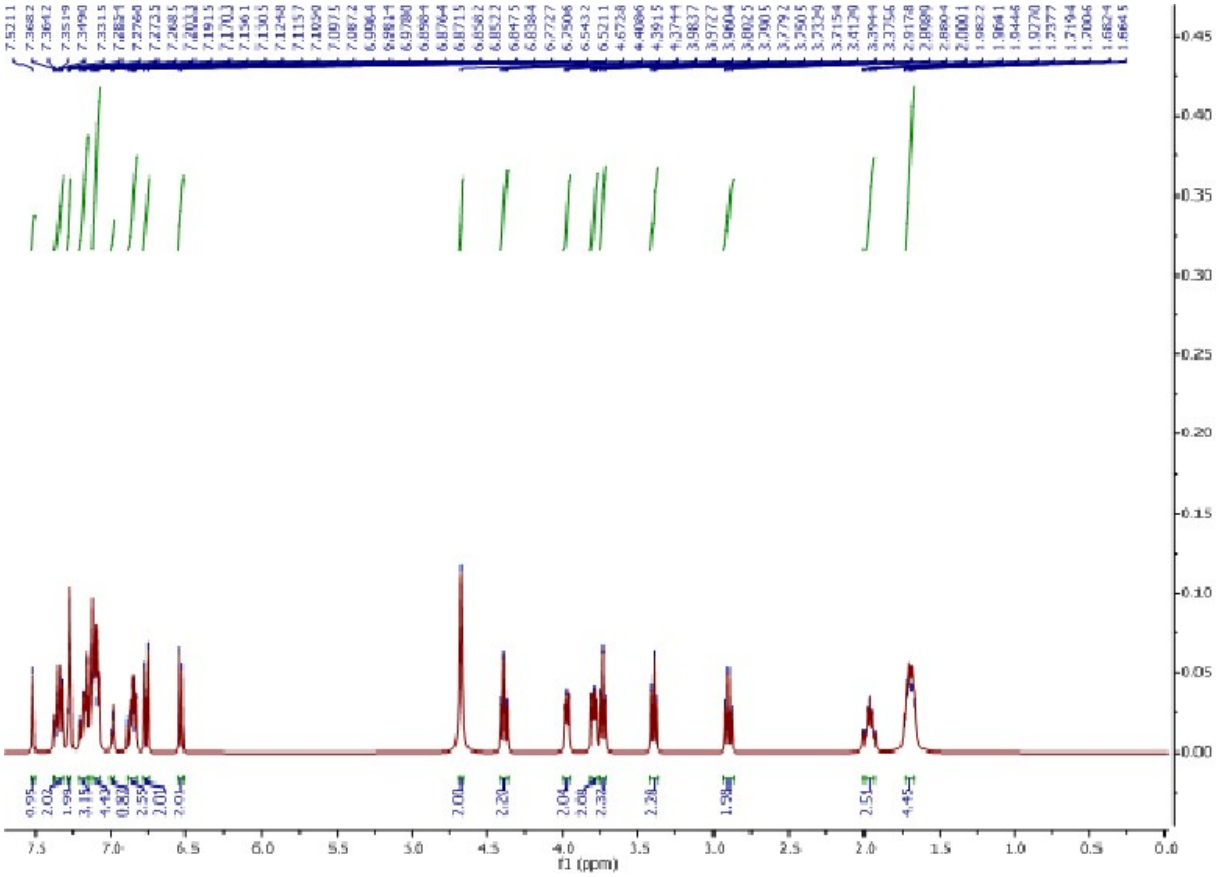

^{1}H NMR aliphatic expansion of (Z)-1-(5-(4-((2-(4(4-choro-1,2-diphenylbut-1-en-1yl)phenoxy)ethoxy)methyl)-1H-1,2,3-triazol-1-yl)pentyl)indoline-2,3-dione (11c):

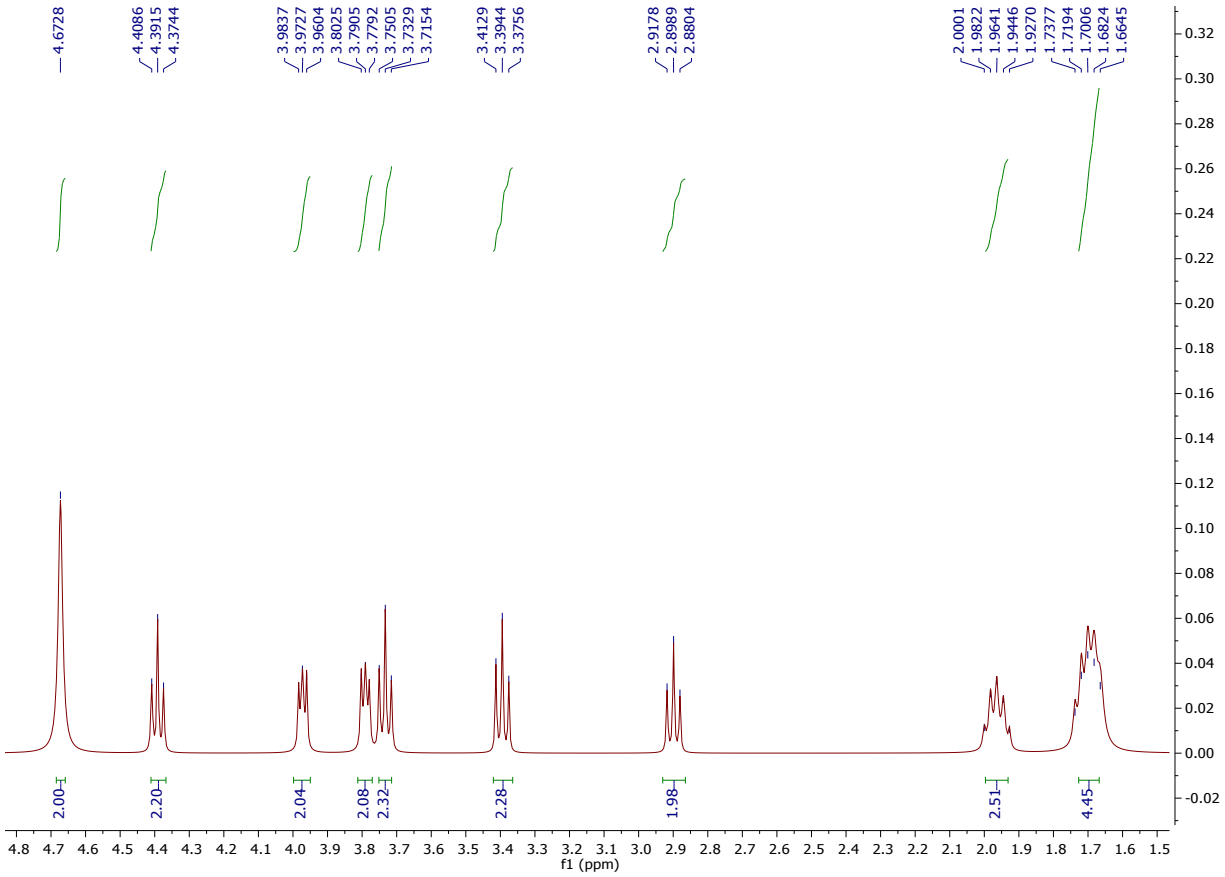

^{1}H NMR aromatic expansion of (Z)-1-(5-(4-((2-(4(4-choro-1,2-diphenylbut-1-en-1yl)phenoxy)ethoxy)methyl)-1H-1,2,3-triazol-1-yl)pentyl)indoline-2,3-dione (11c):

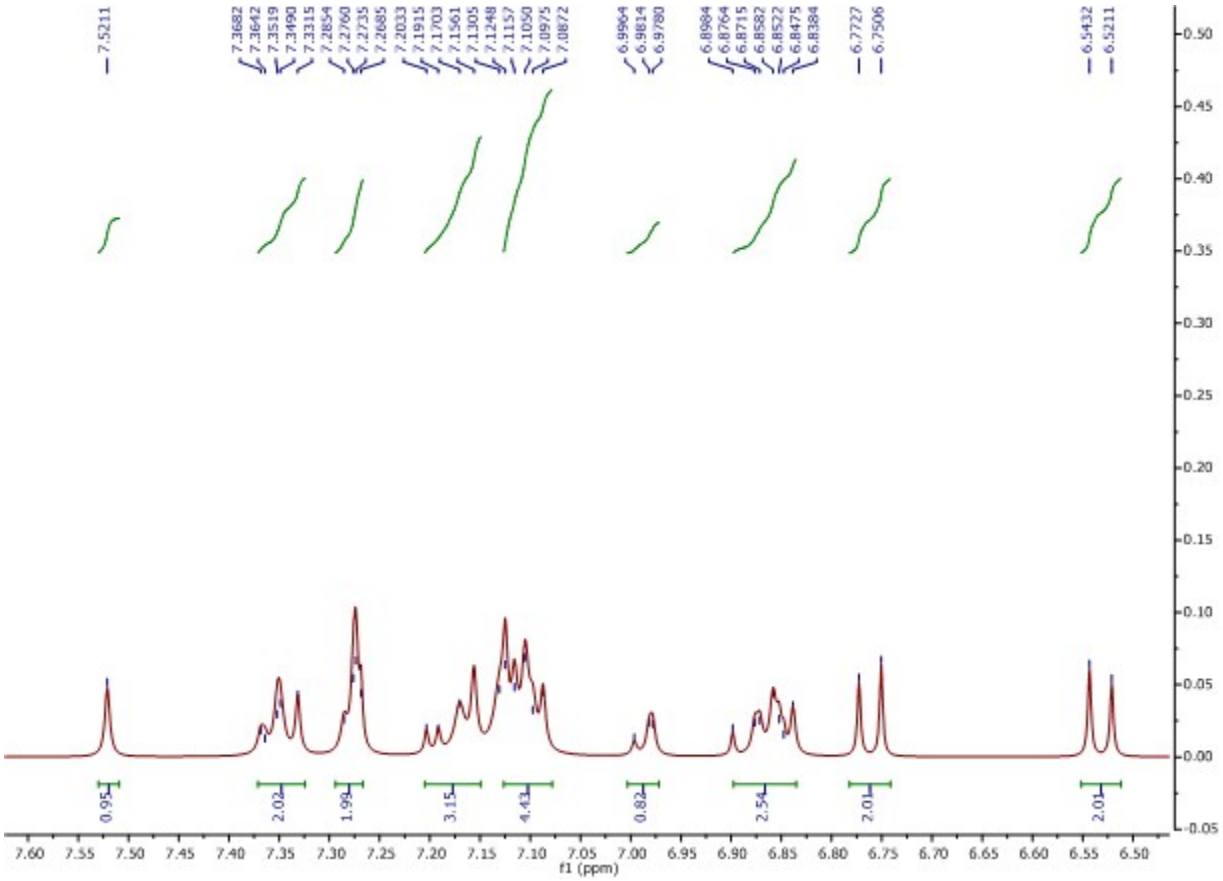

^{13}C NMR of (Z)-1-(5-(4-((2-(4(4-choro-1,2-diphenylbut-1-en-1yl)phenoxy)ethoxy)methyl)-1H-1,2,3-triazol-1-yl)pentyl)indoline-2,3-dione (11c):

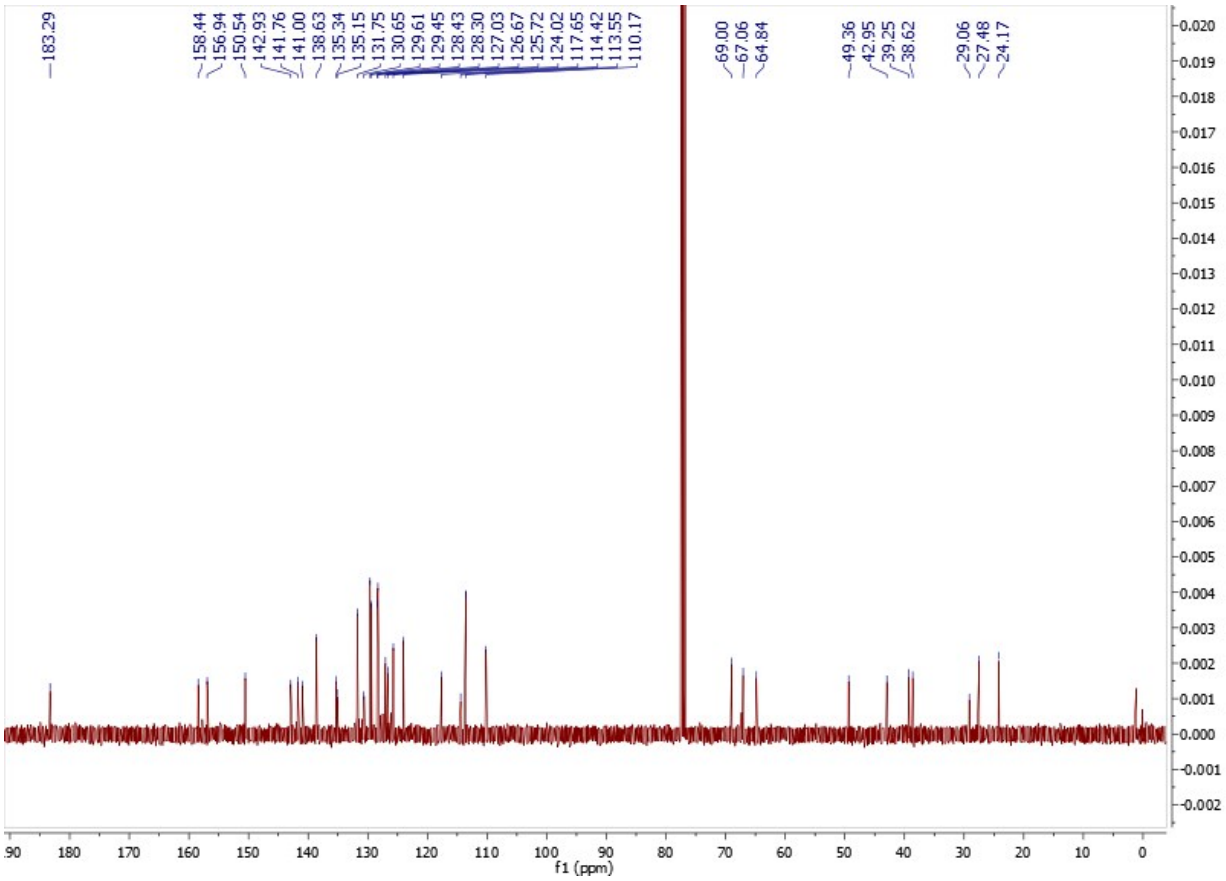

^{1}H NMR of (Z)-1-(8-(4-((2-(4-choro-1,2-diphenylbut-1-en-1yl)phenoxy)ethoxy)methyl)-1H-1,2,3-triazol-1-yl)octyl)indoline-2,3-dione (11d):

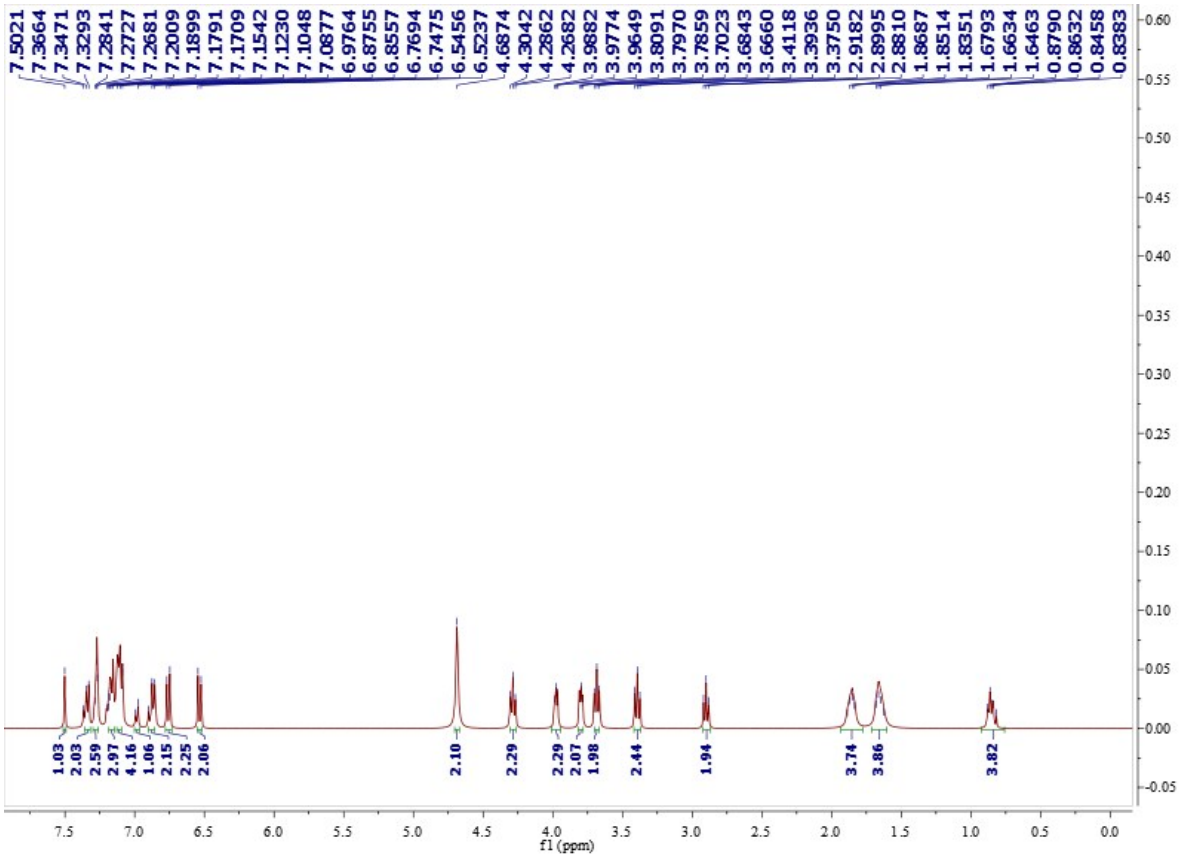

^{13}C NMR of (Z)-1-(8-(4-((2-(4-choro-1,2-diphenylbut-1-en-1yl)phenoxy)ethoxy)methyl)-1H-1,2,3-triazol-1-yl)octyl)indoline-2,3-dione (11d):

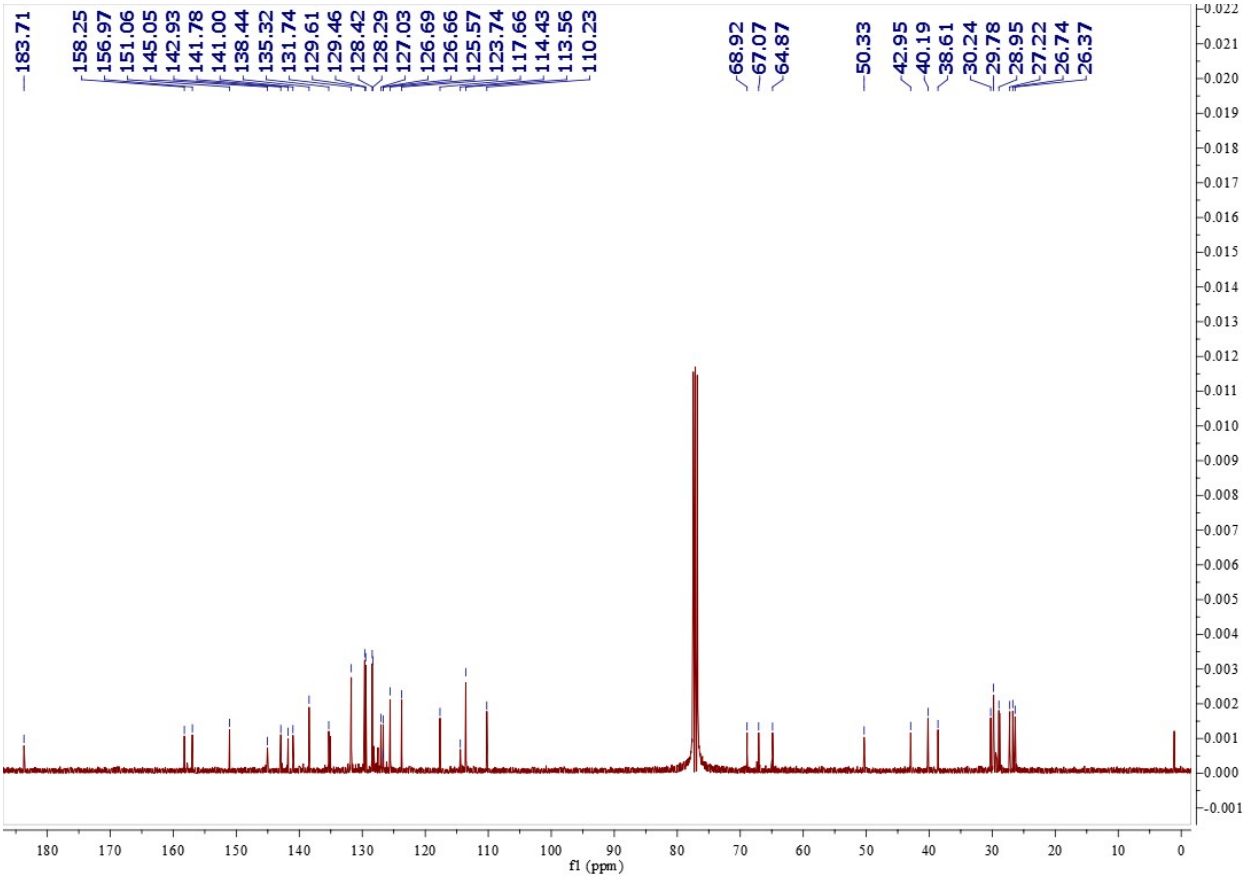

^{1}H NMR of (Z)-1-(3-(4-((2-(4-(4-choro-1,2-diphenylbut-1-en-1yl)phenoxy)ethoxy)methyl)-1H-1,2,3-triazol-1-yl)propyl)indoline-2,3-dione (11e):

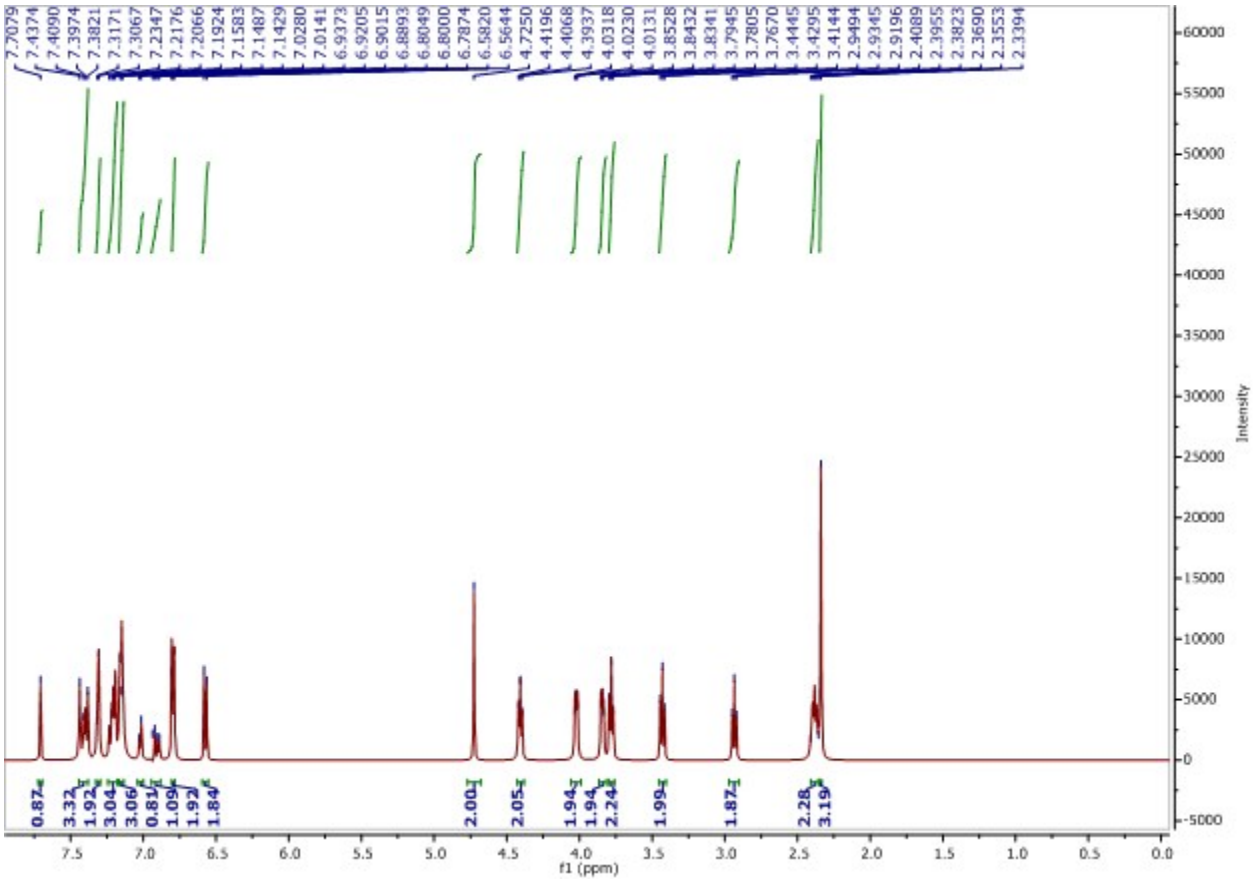

^{13}C NMR of (Z)-1-(3-(4-((2-(4-(4-choro-1,2-diphenylbut-1-en-1yl)phenoxy)ethoxy)methyl)-1H-1,2,3-triazol-1-yl)propyl)indoline-2,3-dione (11e):

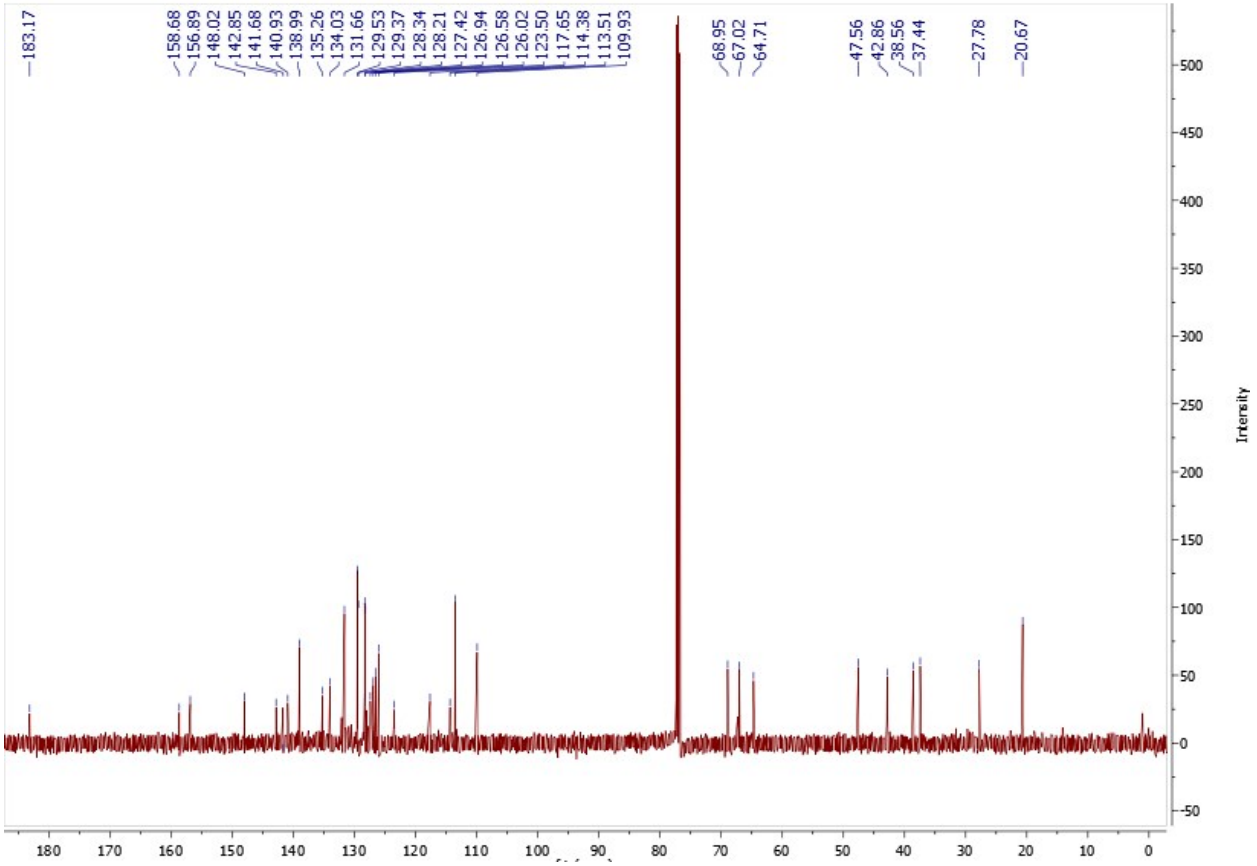

^{1}H NMR of (Z)-5-chloro-1-(3-(4-((2-(4-(4-chloro-1,2-diphenylbut-1-en-1-yl)phenoxy)ethoxy)methyl)-1*H*-1,2,3-triazol-1-yl)propyl)indoline-2,3-dione (11f):

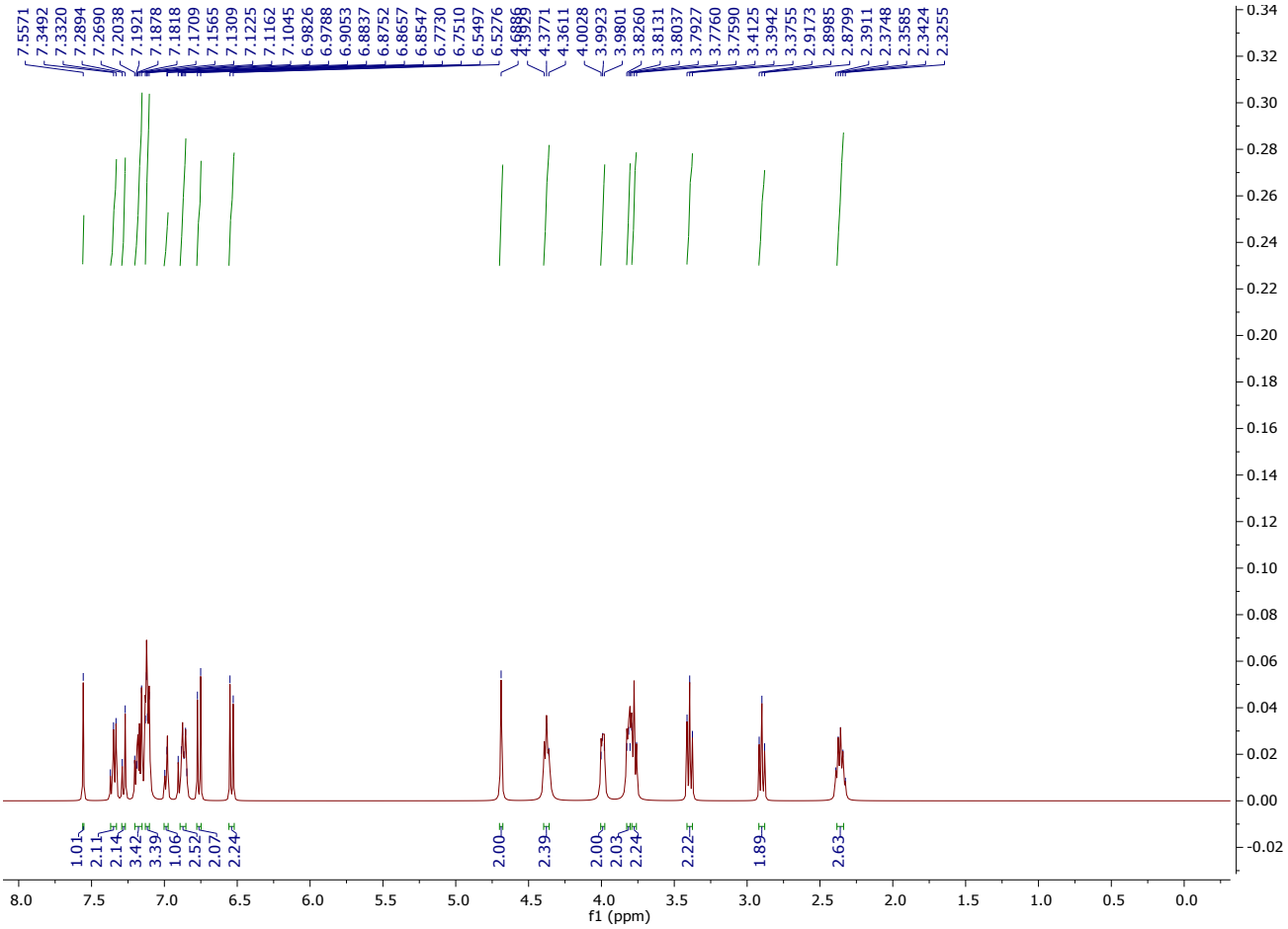

^{1}H NMR aliphatic expansion of (Z)-5-chloro-1-(3-(4-((2-(4-(4-chloro-1,2-diphenylbut-1-en-1-yl)phenoxy)ethoxy)methyl)-1*H*-1,2,3-triazol-1-yl)propyl)indoline-2,3-dione (11f):

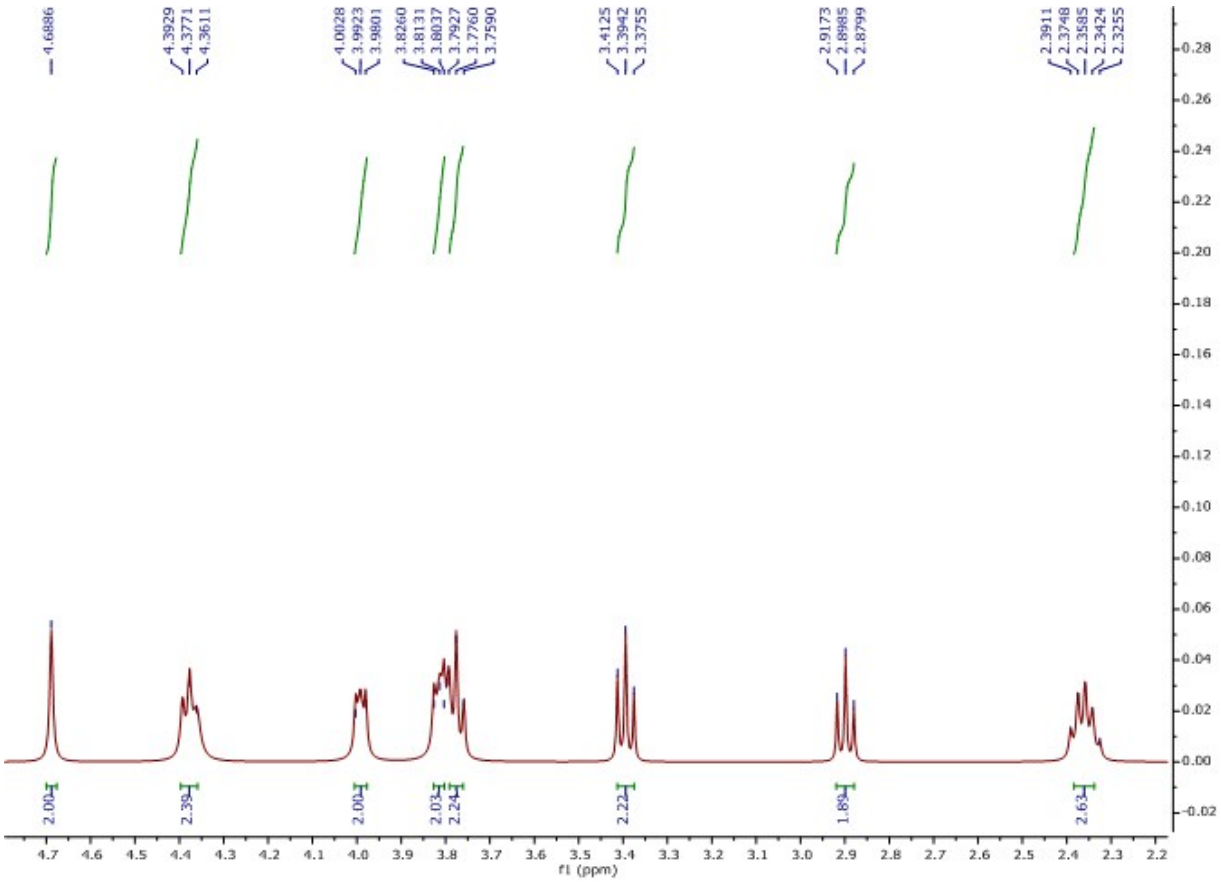

^{1}H NMR aromatic expansion of (Z)-5-chloro-1-(3-(4-((2-(4-(4-chloro-1,2-diphenylbut-1-en-1-yl)phenoxy)ethoxy)methyl)-1*H*-1,2,3-triazol-1-yl)propyl)indoline-2,3-dione (11f):

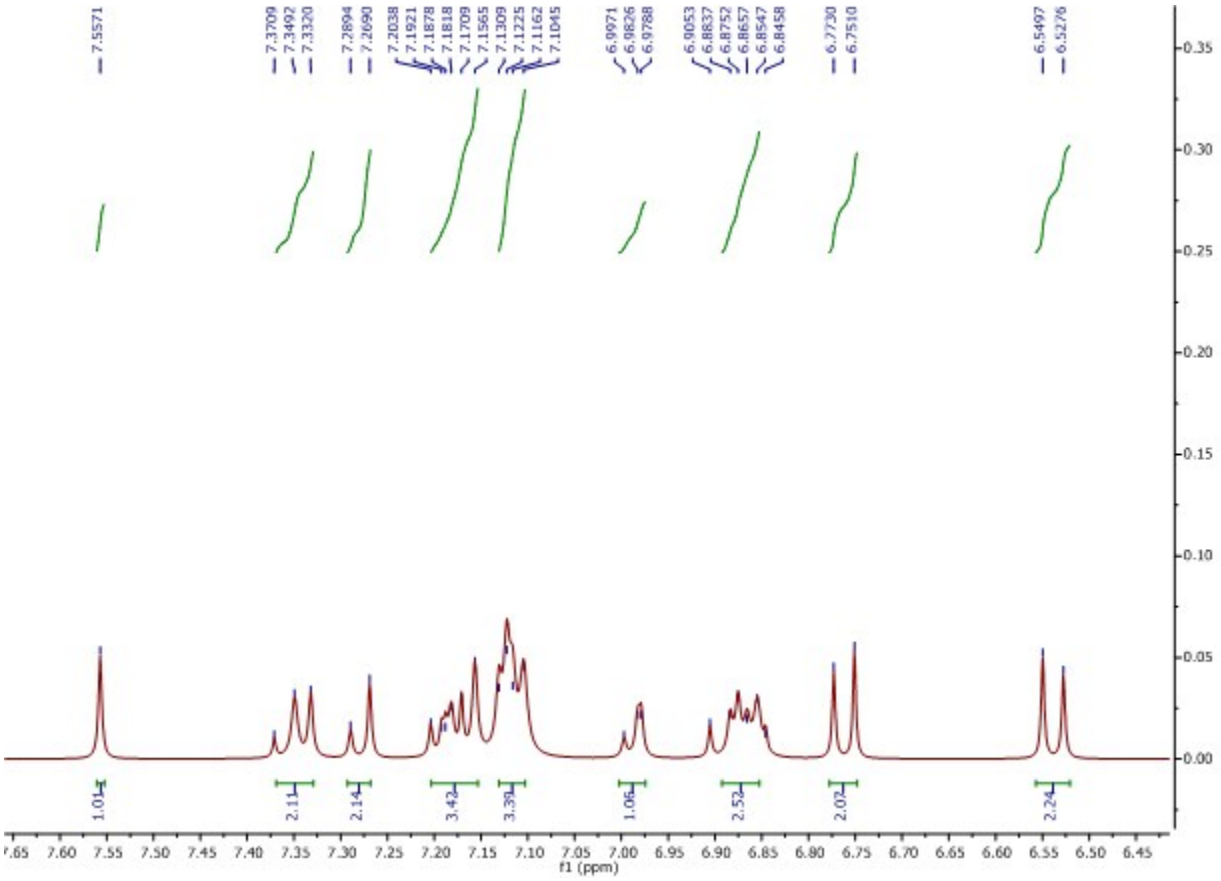

^{13}C NMR of (Z)-5-chloro-1-(3-(4-((2-(4-(4-chloro-1,2-diphenylbut-1-en-1-yl)phenoxy)ethoxy)methyl)-1*H*-1,2,3-triazol-1-yl)propyl)indoline-2,3-dione (11f):

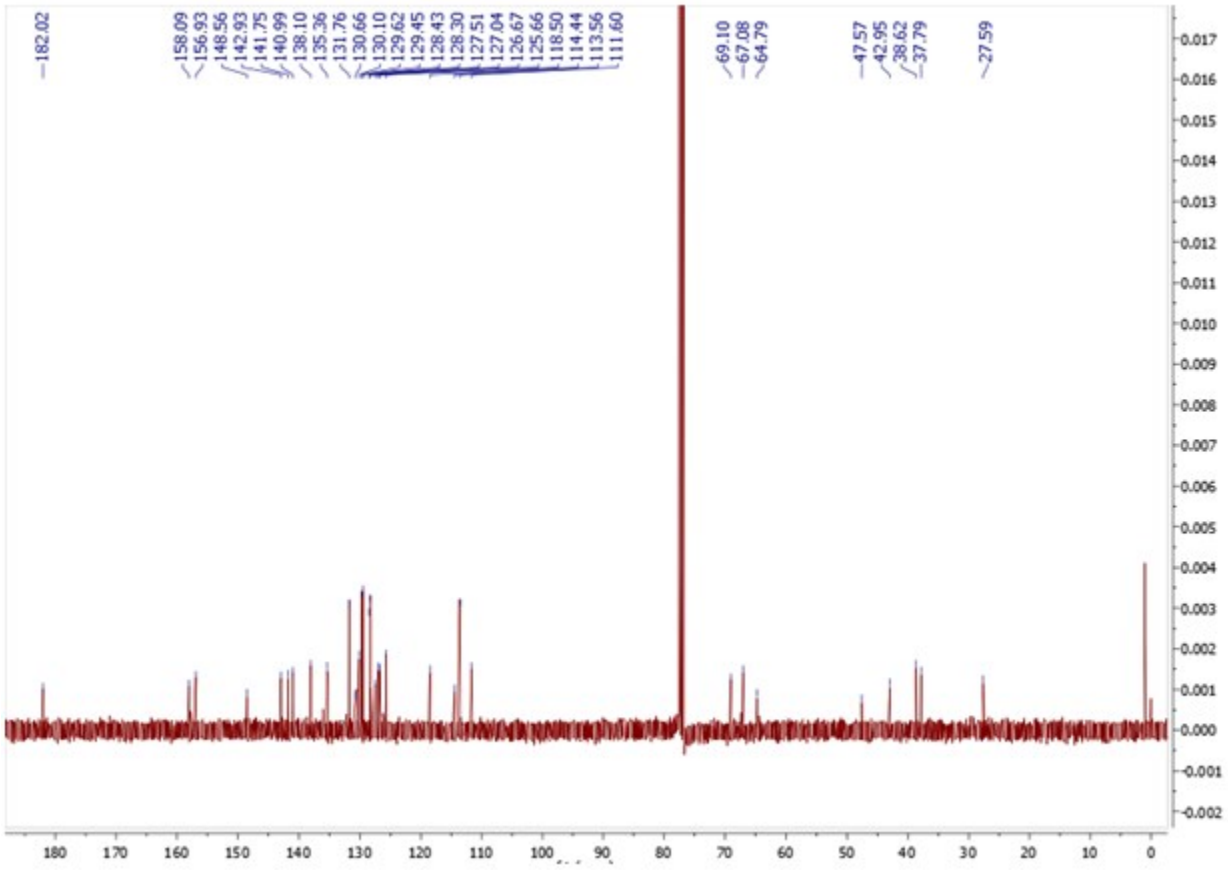

^{1}H NMR of (Z)-1-(4-(4-((2-(4-(4-chloro-1,2-diphenylbut-1-en-1-yl)phenoxy)ethoxy)methyl)-1H-1,2,3-triazol-1-yl)butyl)-5-fluoroindoline-2,3-dione (11i):

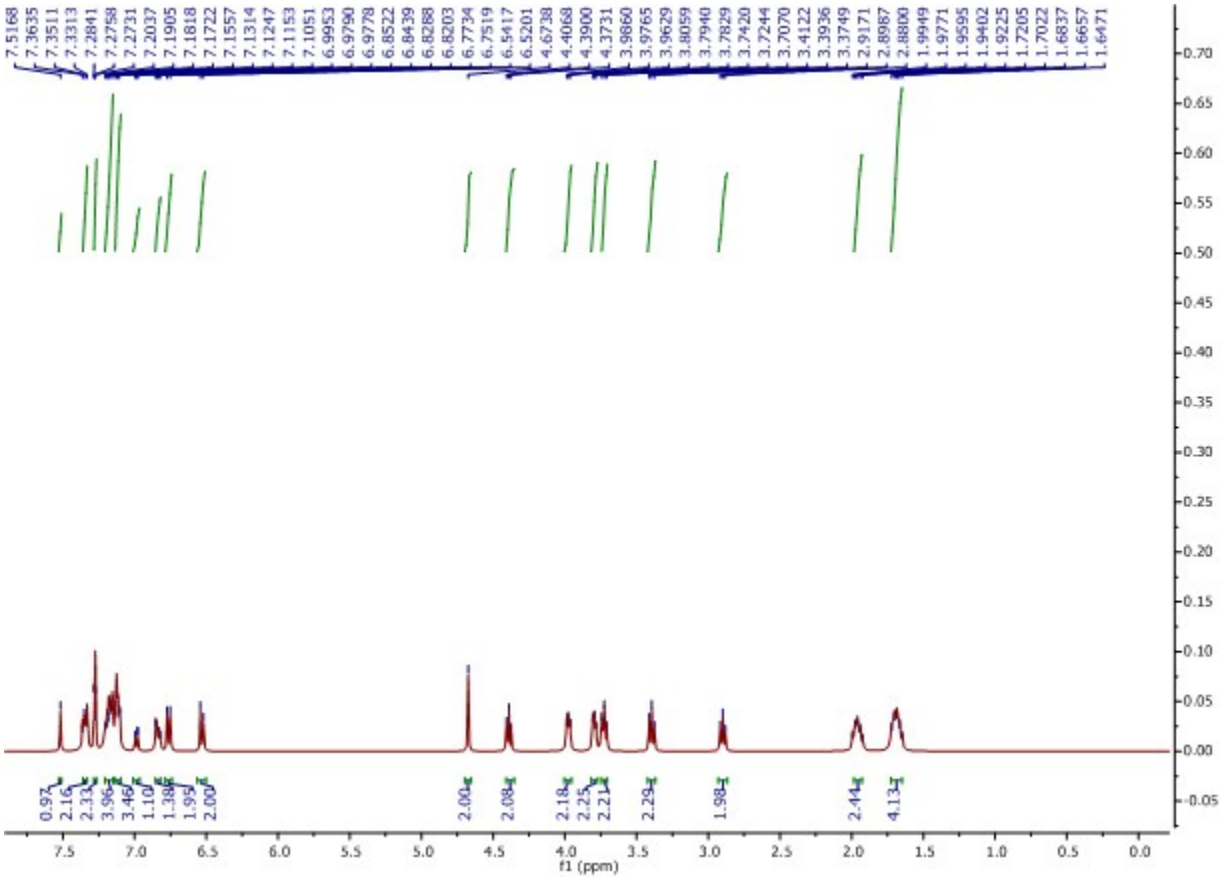

^{13}C NMR of (Z)-1-(4-(4-((2-(4-(4-chloro-1,2-diphenylbut-1-en-1-yl)phenoxy)ethoxy)methyl)-1H-1,2,3-triazol-1-yl)butyl)-5-fluoroindoline-2,3-dione (11i):

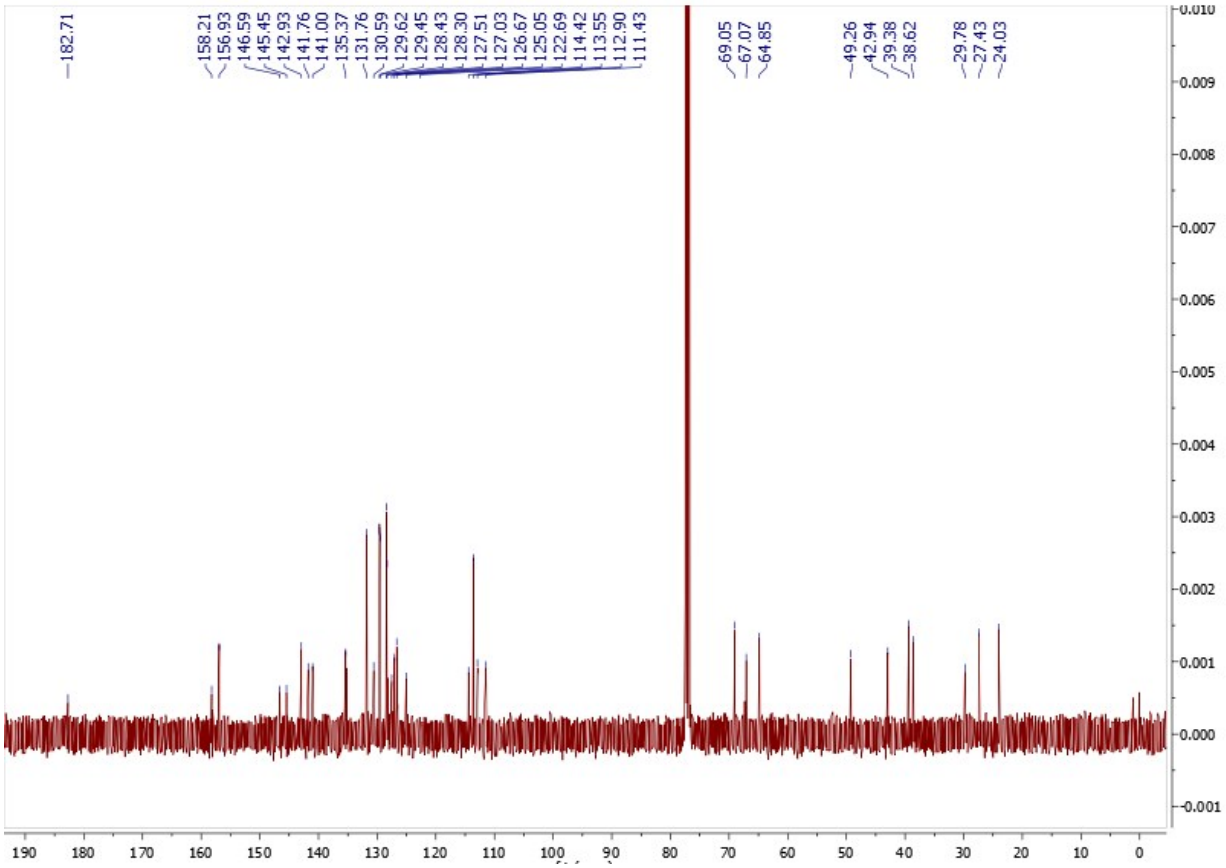

^{1}H NMR of (Z)-5,7-dibromo-1-(2-(4-((2-(4-(4-chloro-1,2-diphenylbut-1-en-1-yl)phenoxy)ethoxy)methyl)-1H-1,2,3-triazol-1-yl)ethyl)indoline-2,3-dione (11j):

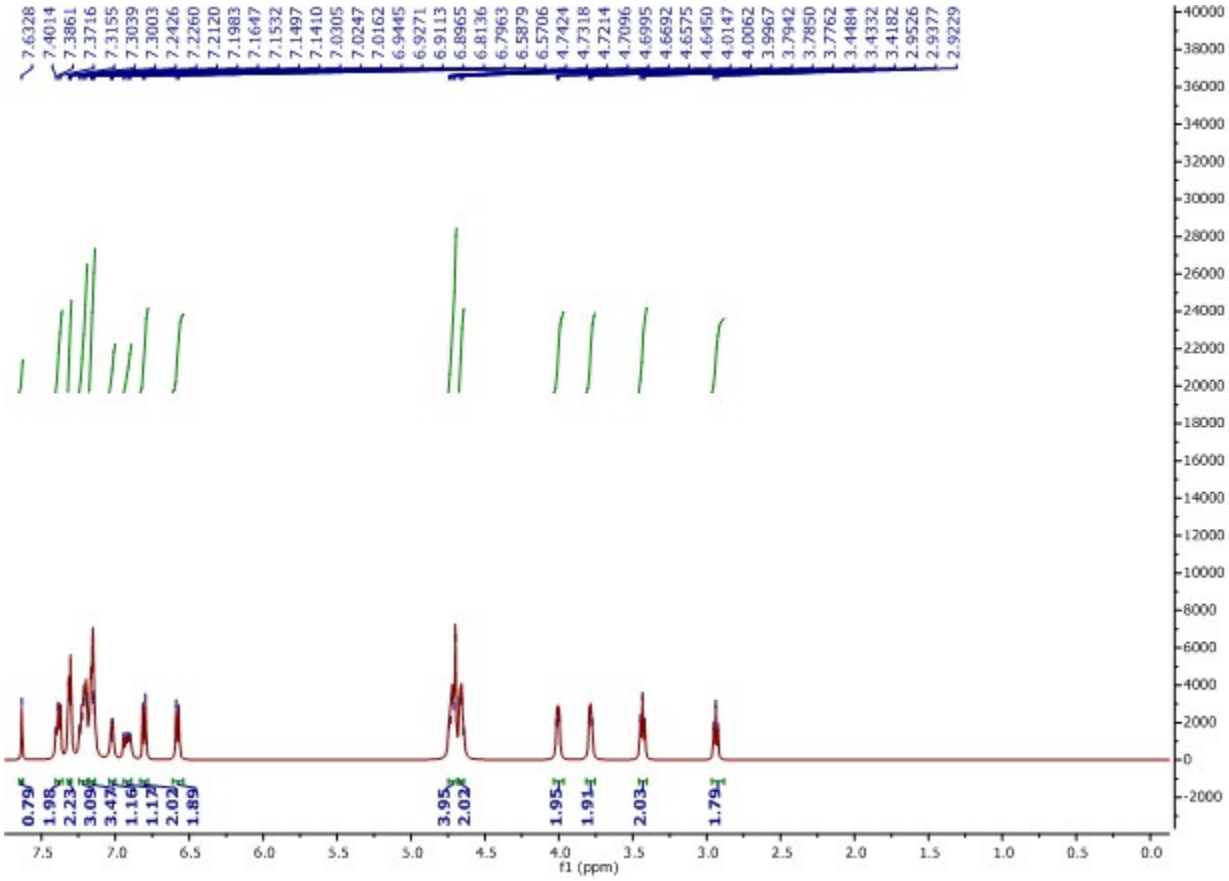

^{13}C NMR of (Z)-5,7-dibromo-1-(2-(4-((2-(4-(4-chloro-1,2-diphenylbut-1-en-1-yl)phenoxy)ethoxy)methyl)-1H-1,2,3-triazol-1-yl)ethyl)indoline-2,3-dione (11j):

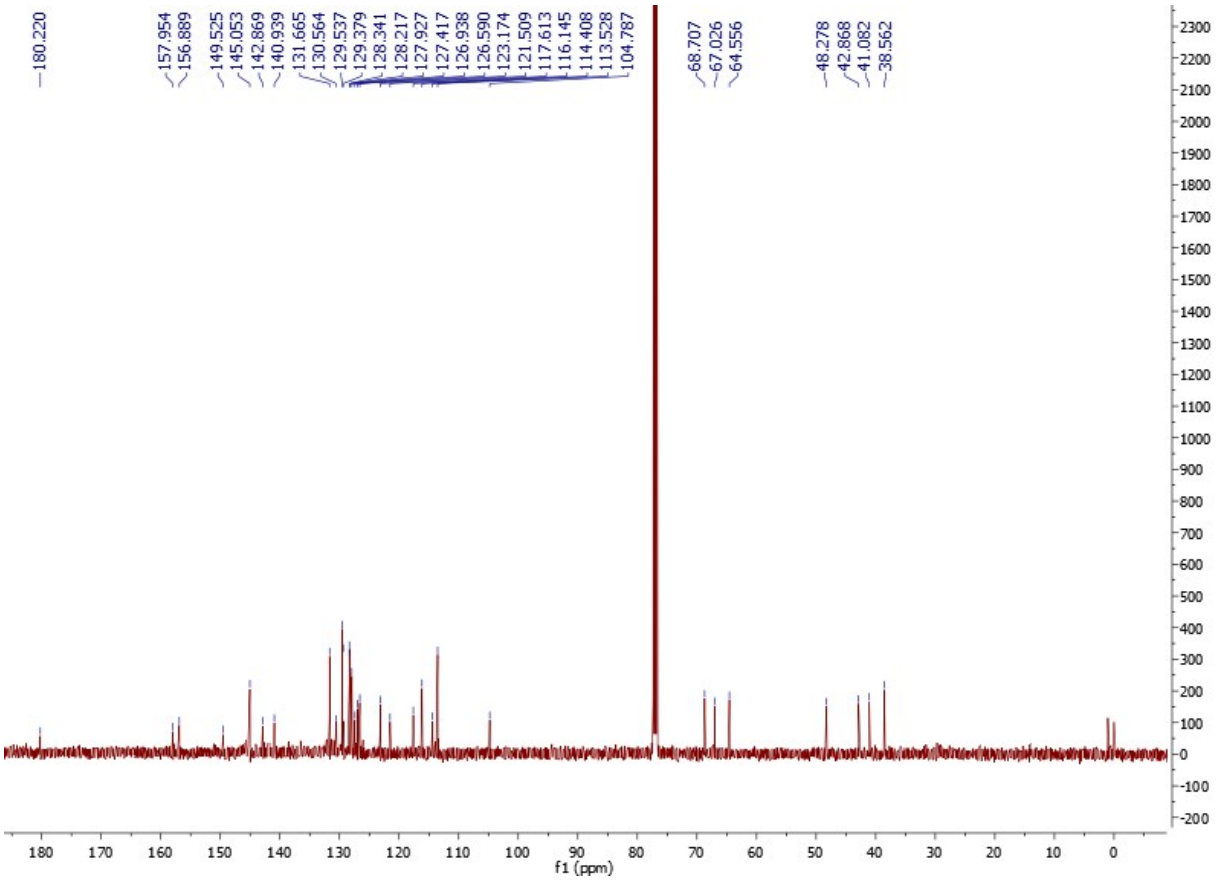

^{1}H NMR of (Z)-5,7-dibromo-1-(4-(4-((2-(4-(4-chloro-1,2-diphenylbut-1-en-1-yl)phenoxy)ethoxy)methyl)-1H-1,2,3-triazol-1-yl)butyl)indoline-2,3-dione (11l):

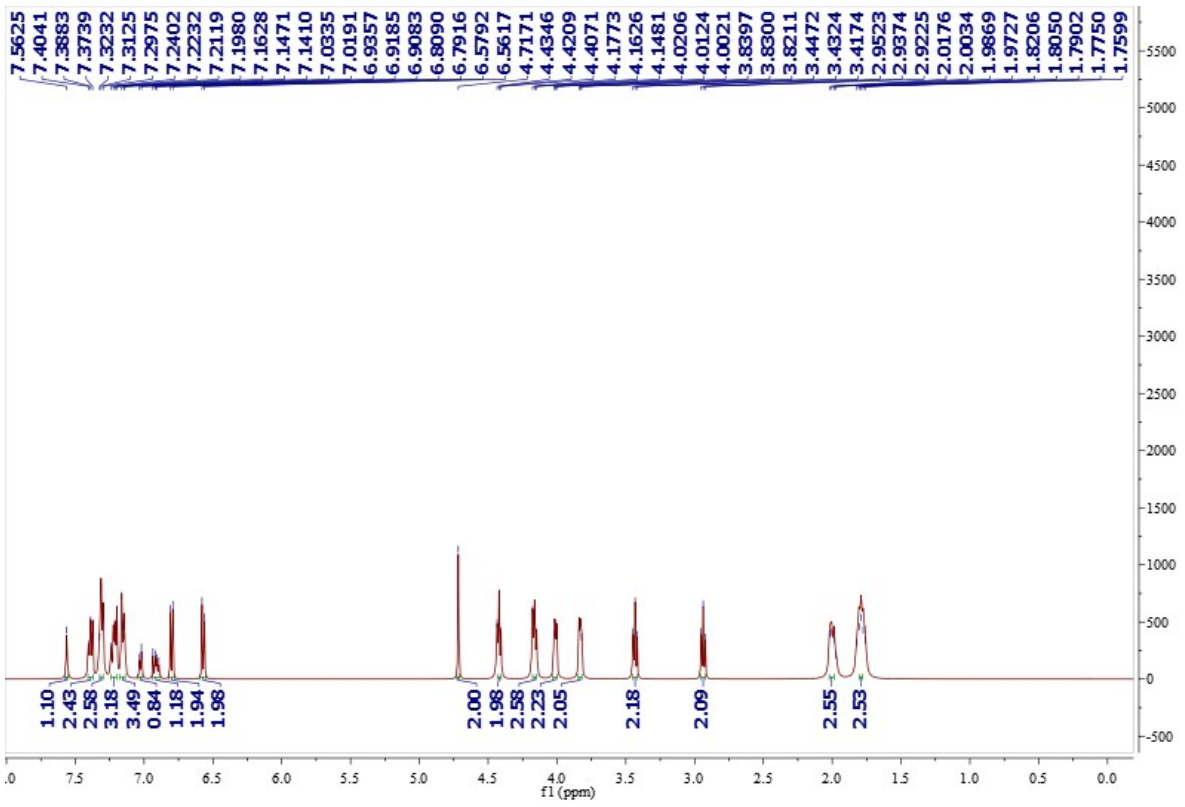

^{13}C NMR of (Z)-5,7-dibromo-1-(4-(4-((2-(4-(4-chloro-1,2-diphenylbut-1-en-1-yl)phenoxy)ethoxy)methyl)-1H-1,2,3-triazol-1-yl)butyl)indoline-2,3-dione (11l)

:

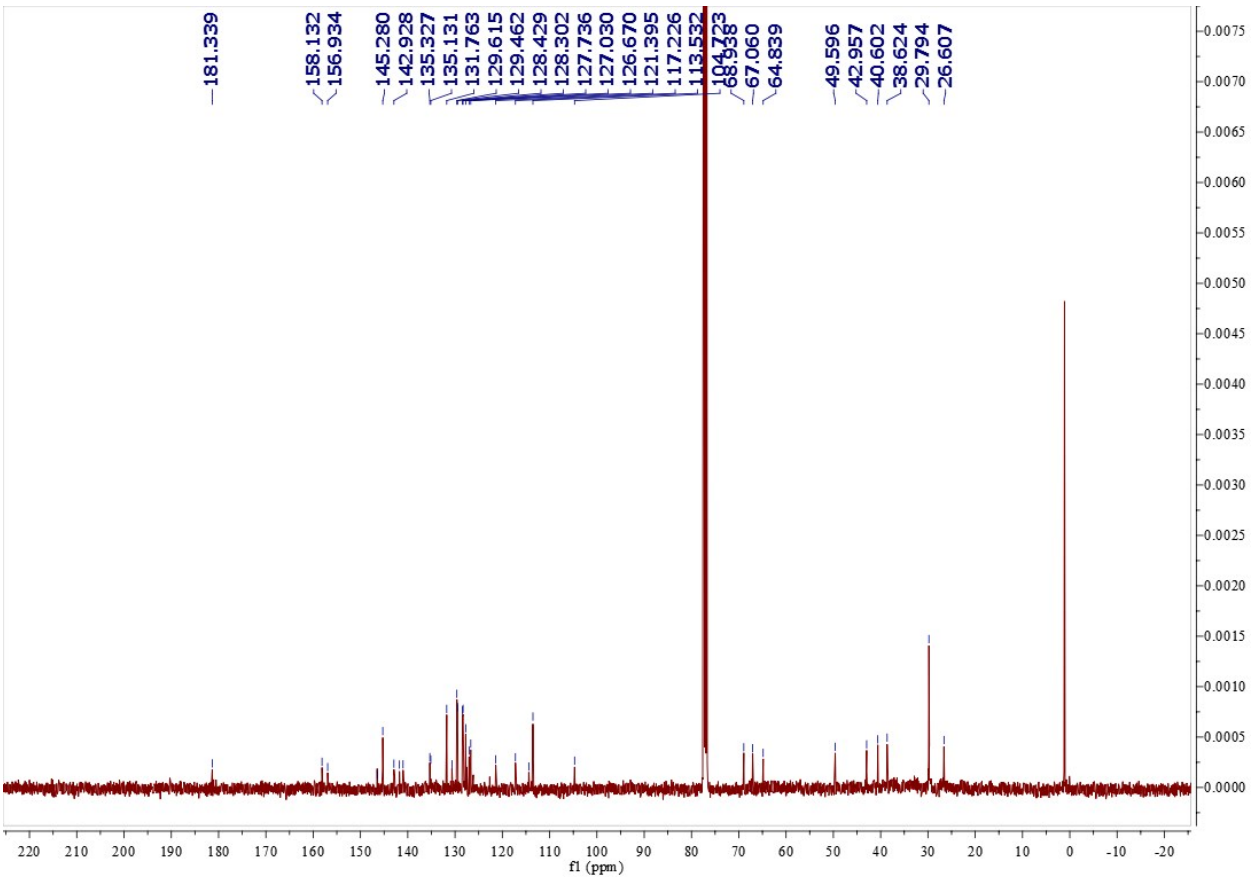

Expanded Aromatic Region of 11l:

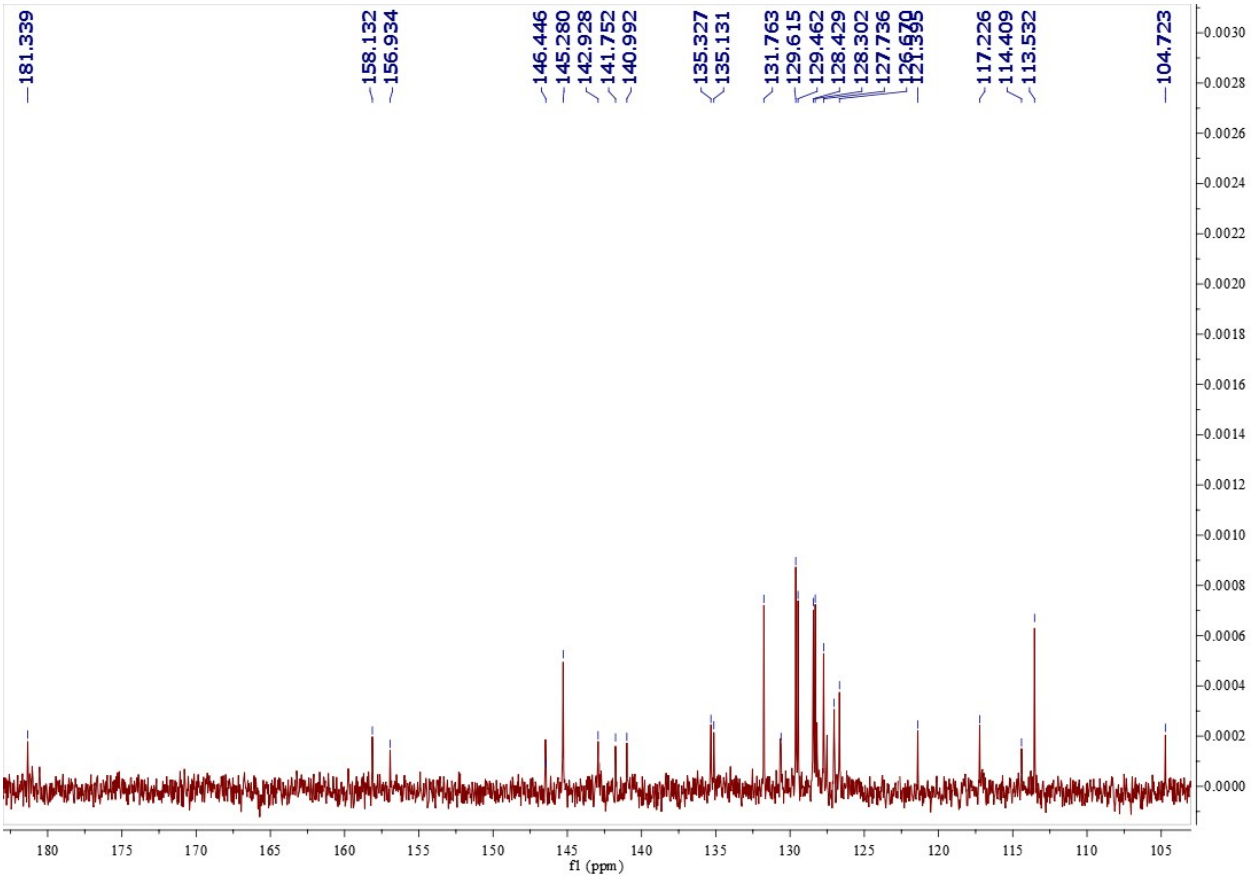

^{1}H NMR of (Z)-1-(5-(4-((2-(4-(4-chloro-1,2-diphenylbut-1-en-1-yl)phenoxy)ethoxy)methyl-1H-1,2,3-trazol-1-yl)pentyl)spiro[indoline-3,2'-[1,3]dioxolan]-2-one (12a)

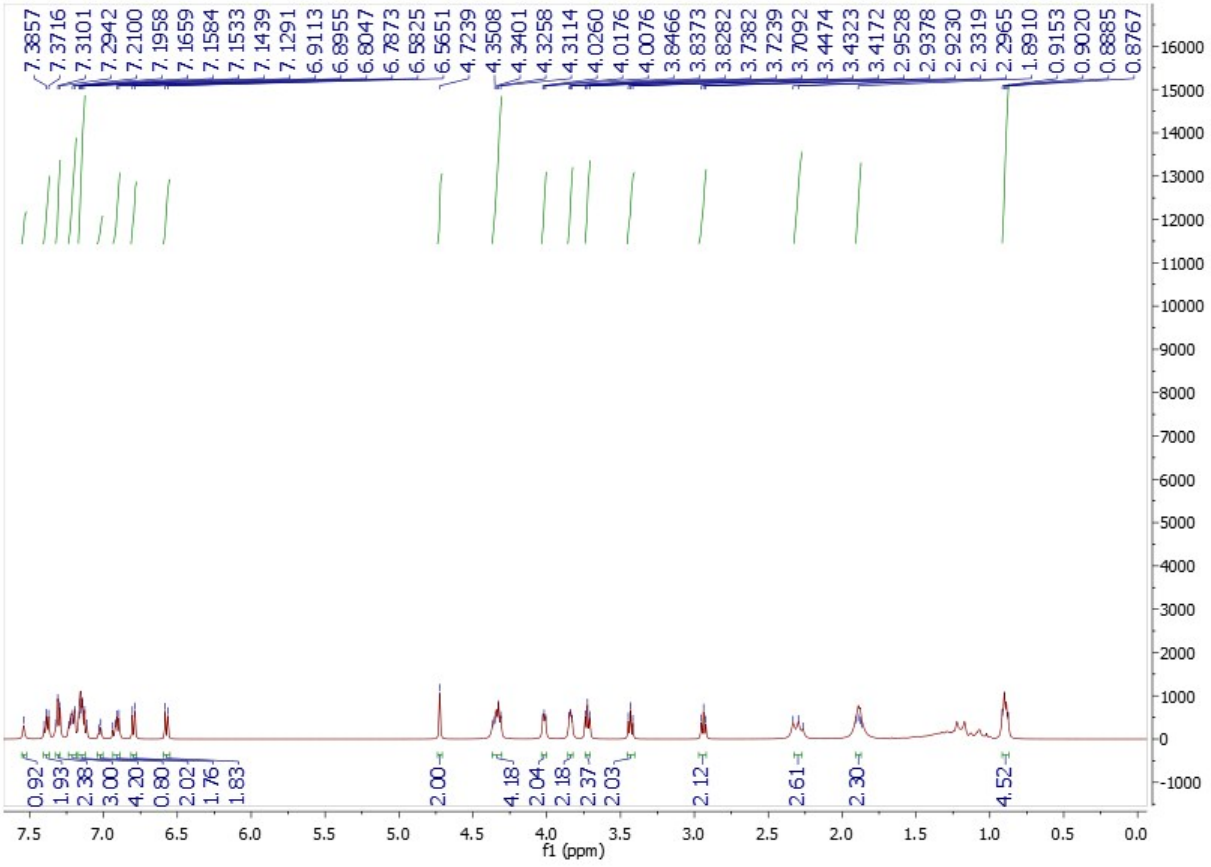

^{1}H NMR of (Z)-1-(8-(4-((2-(4-(4-chloro-1,2-diphenylbut-1-en-1-yl)phenoxy)ethoxy)methyl-1H-1,2,3-trazol-1-yl)octyl)spiro[indoline-3,2'-[1,3]dioxolan]-2-one (12b):

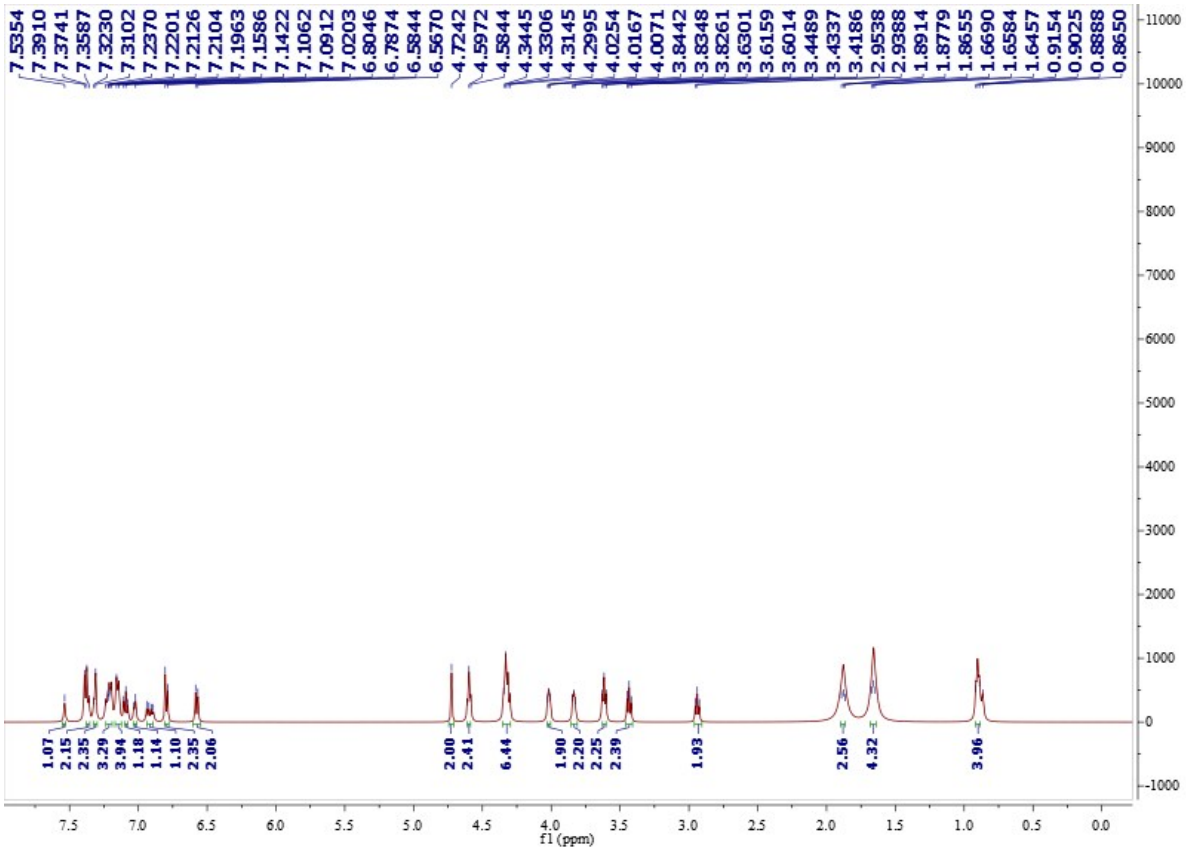

^{13}C NMR of (Z)-1-(8-(4-((2-(4-(4-chloro-1,2-diphenylbut-1-en-1-yl)phenoxy)ethoxy)methyl-1H-1,2,3-trazol-1-yl)octyl)spiro[indoline-3,2'-[1,3]dioxolan]-2-one (12b):

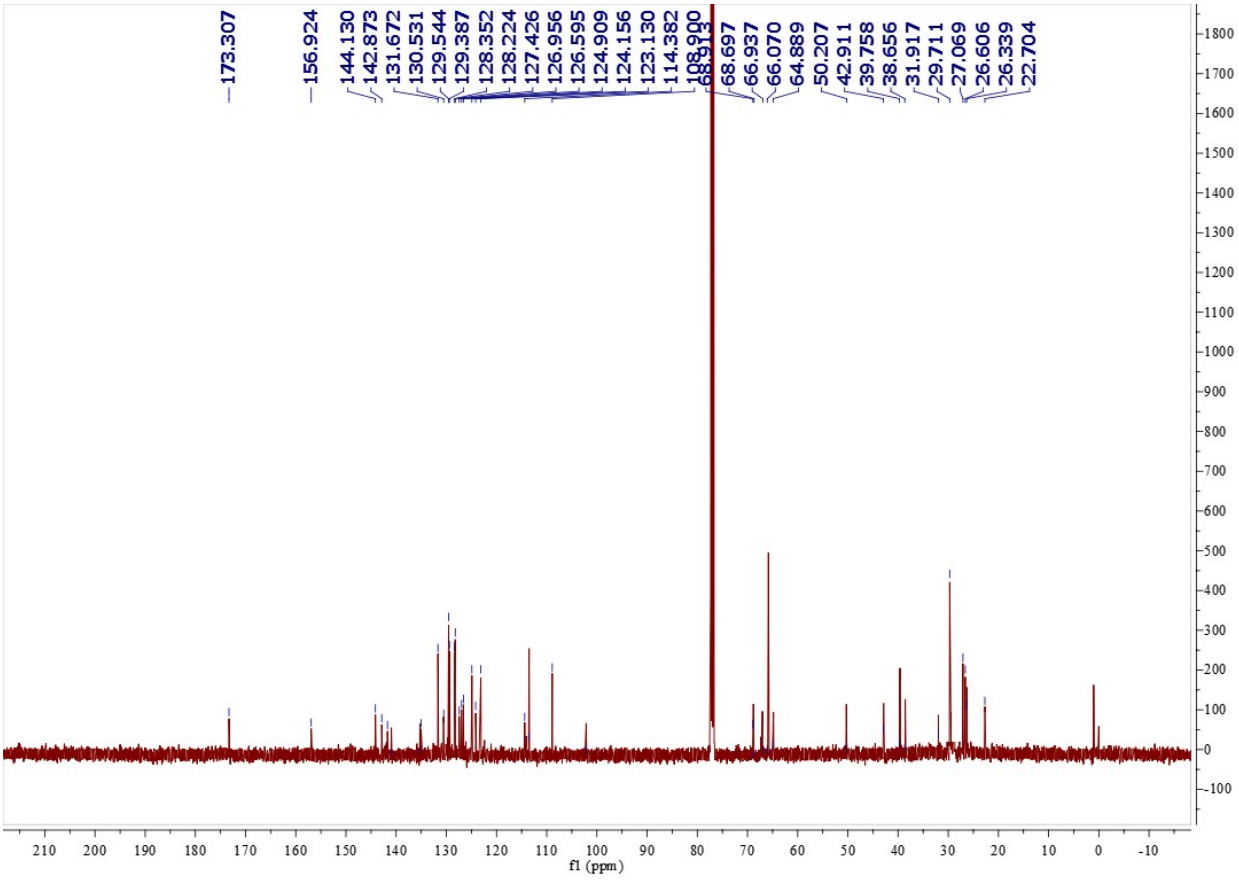

Expanded Aromatic Region of 12b

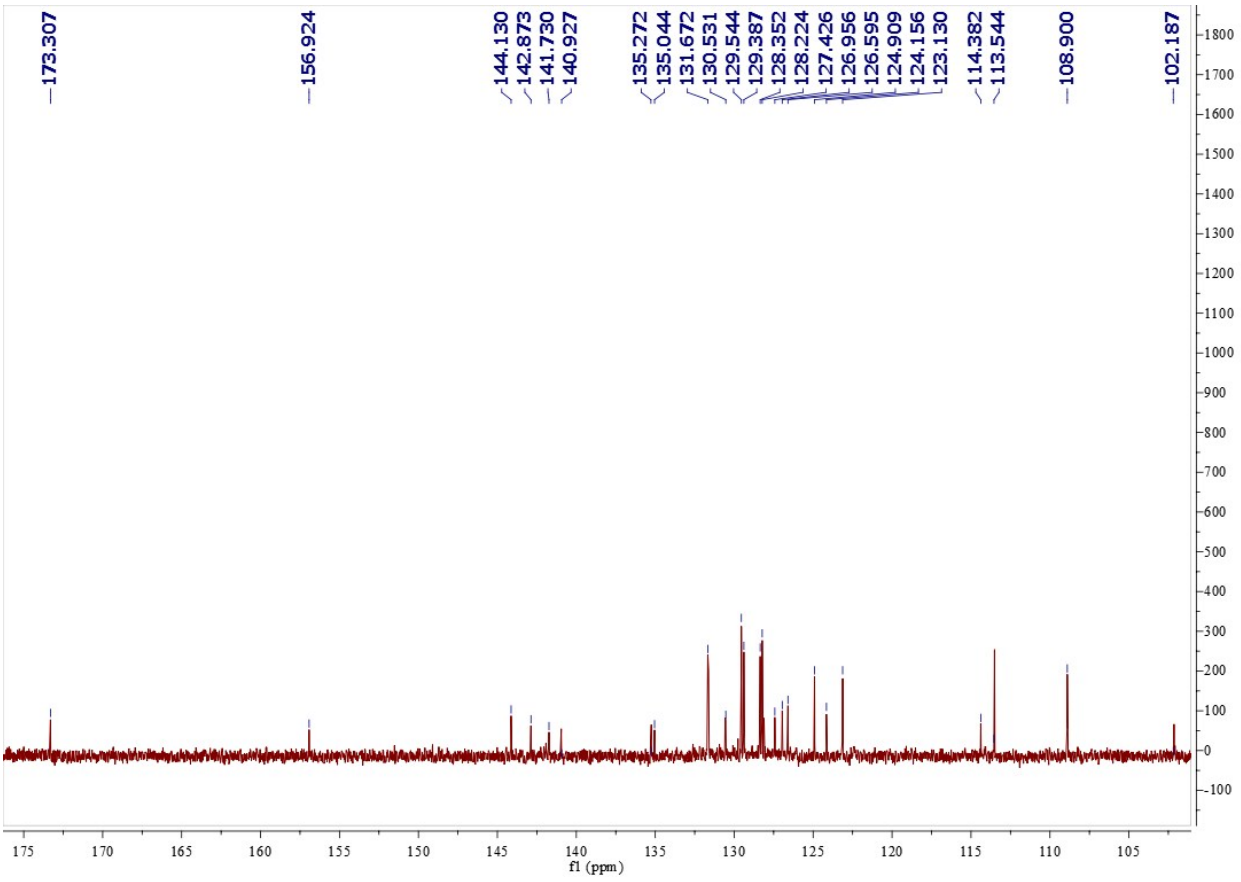

^{1}H NMR of (Z)-5-chloro-1-(3-(4-((2-(4-(4-chloro-1,2-diphenylbut-1-en-1-yl)phenoxy)ethoxy)methyl-1*H*-1,2,3-trazol-1-yl)propyl)spiro[indoline-3,2'-[1,3]dioxolan]-2-one (12c):

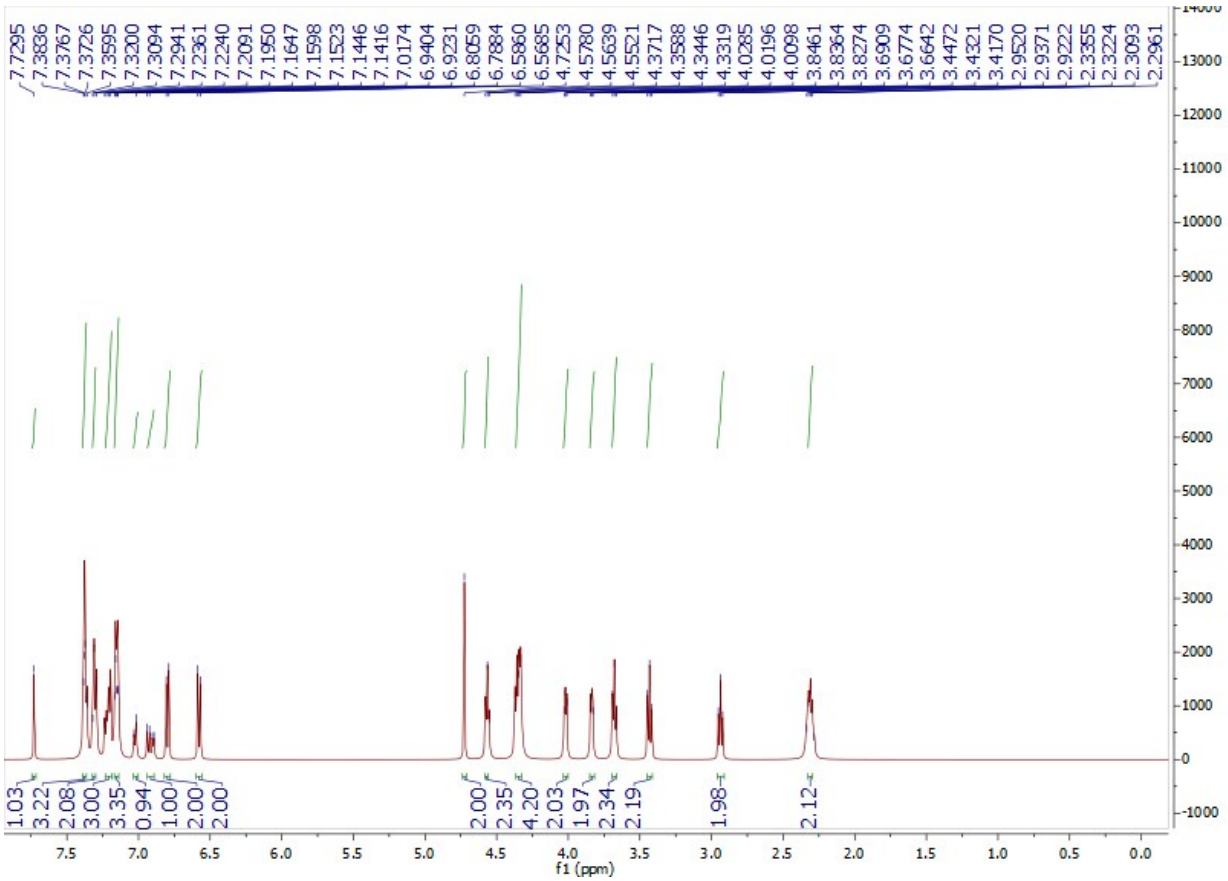

^{13}C NMR of (Z)-5-chloro-1-(3-(4-((2-(4-(4-chloro-1,2-diphenylbut-1-en-1-yl)phenoxy)ethoxy)methyl-1*H*-1,2,3-trazol-1-yl)propyl)spiro[indoline-3,2'-[1,3]dioxolan]-2-one (12c):

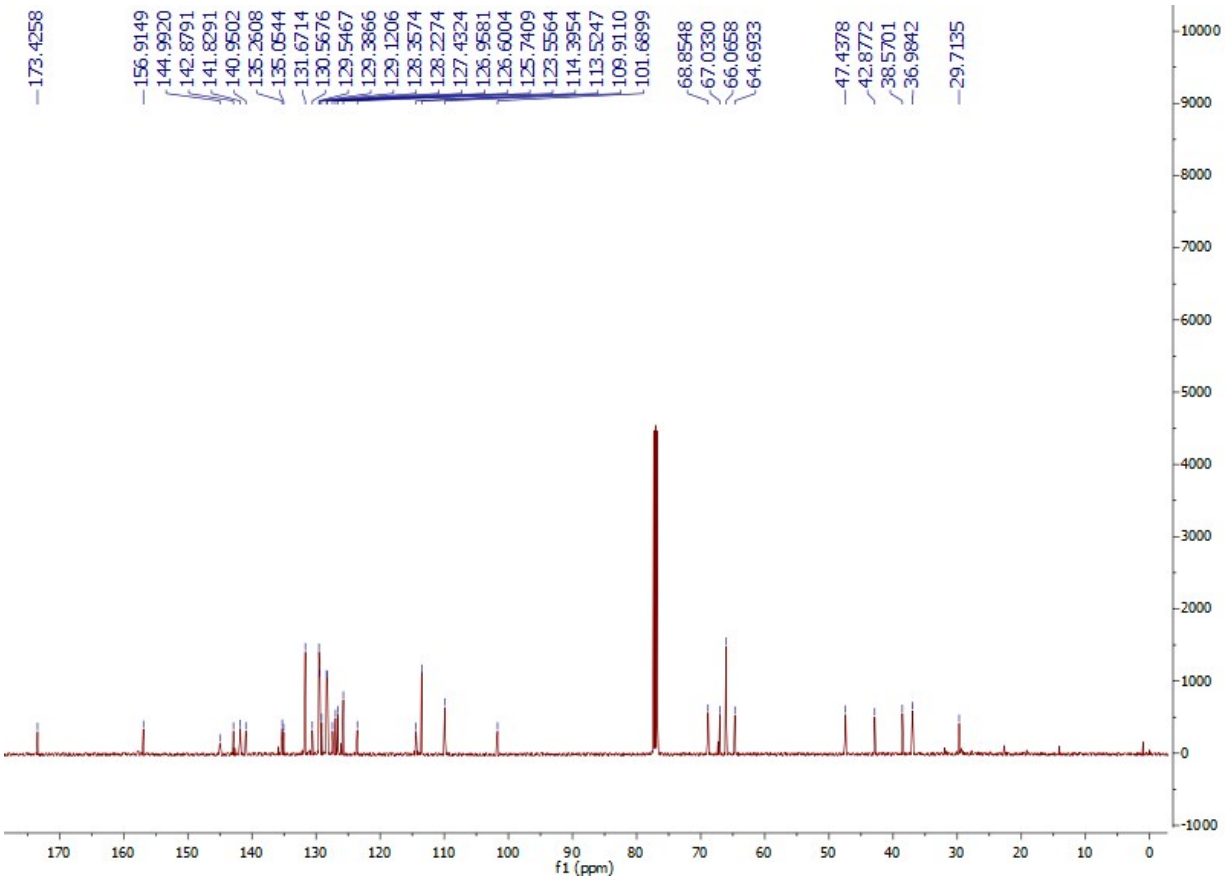

^{1}H NMR of (Z)-5-chloro-1-(6-(4-((2-(4-(4-chloro-1,2-diphenylbut-1-en-1-yl)phenoxy)ethoxy)methyl-1*H*-1,2,3-trazol-1-yl)hexyl)spiro[indoline-3,2'-[1,3]dioxolan]-2-one (12d):

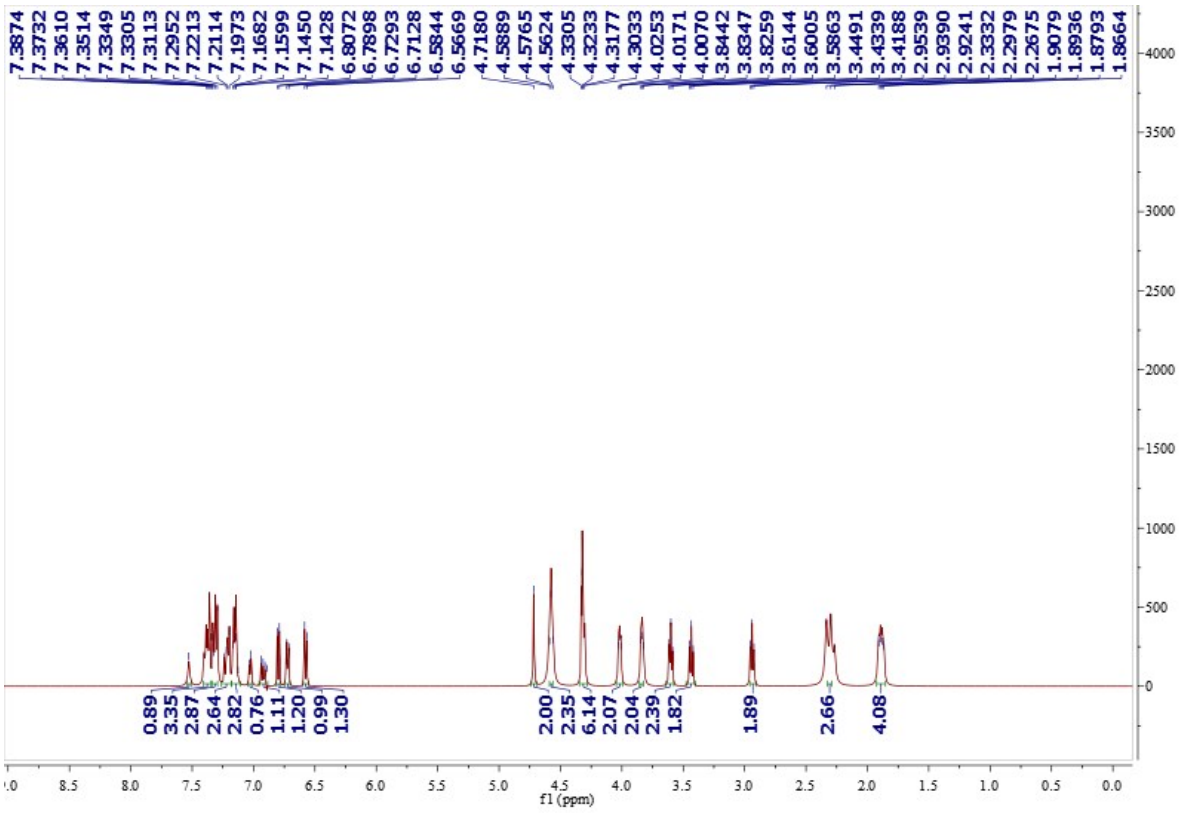

^{13}C NMR of (Z)-5-chloro-1-(6-(4-((2-(4-(4-chloro-1,2-diphenylbut-1-en-1-yl)phenoxy)ethoxy)methyl-1*H*-1,2,3-trazol-1-yl)hexyl)spiro[indoline-3,2'-[1,3]dioxolan]-2-one (12d):

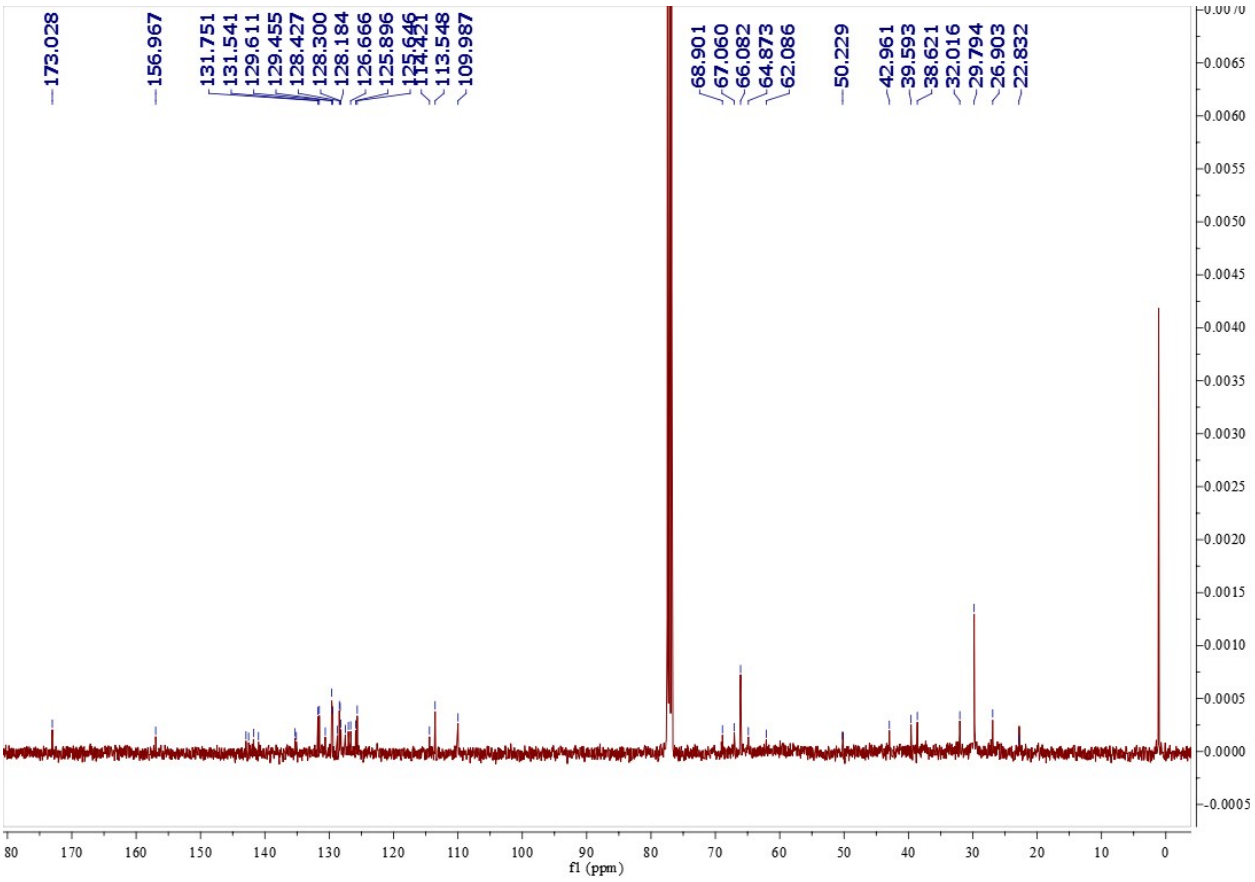

Expanded Aromatic Region of 12d:

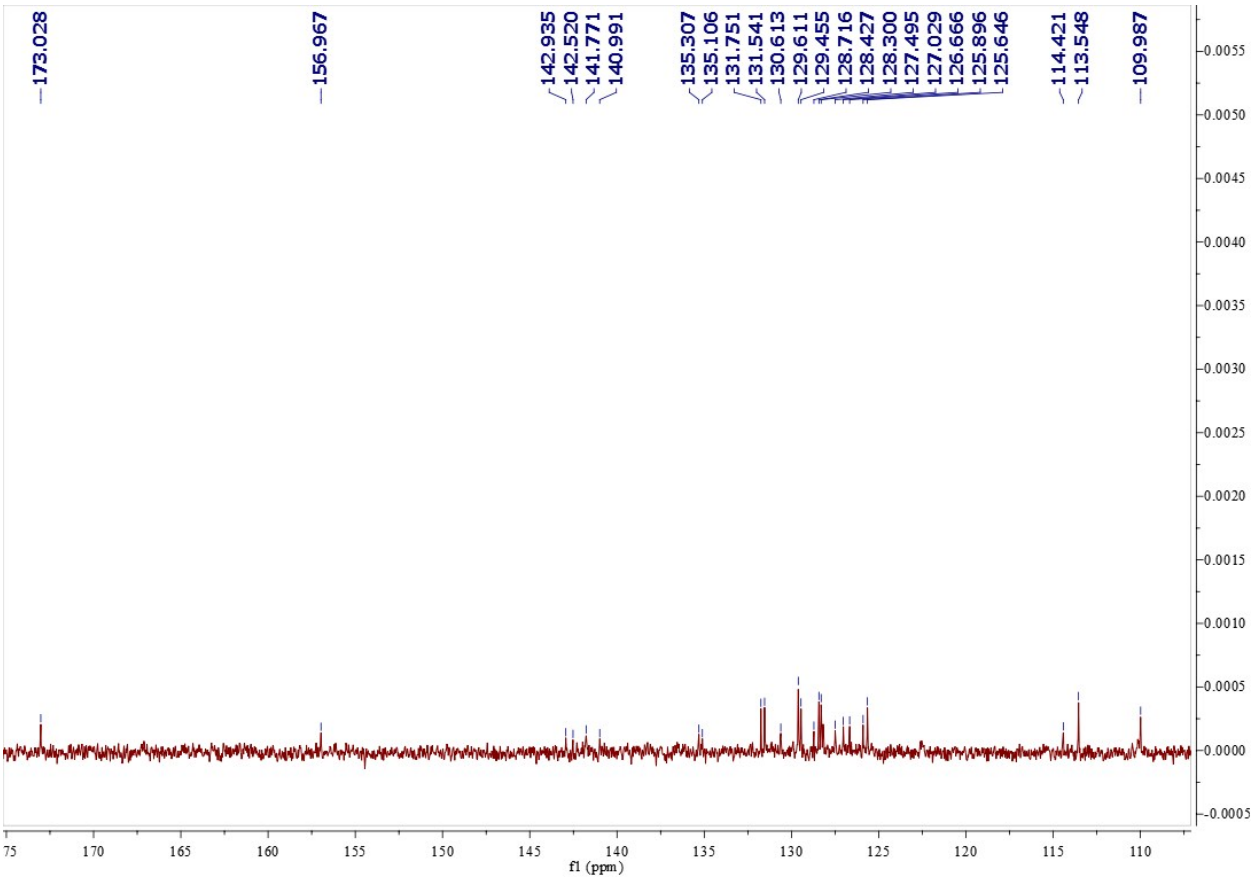

^{1}H NMR of (Z)-5-chloro-1-(8-(4-((2-(4-(4-chloro-1,2-diphenylbut-1-en-1-yl)phenoxy)ethoxy)methyl-1*H*-1,2,3-trazol-1-yl)octyl)spiro[indoline-3,2'-[1,3]dioxolan]-2-one (12e):

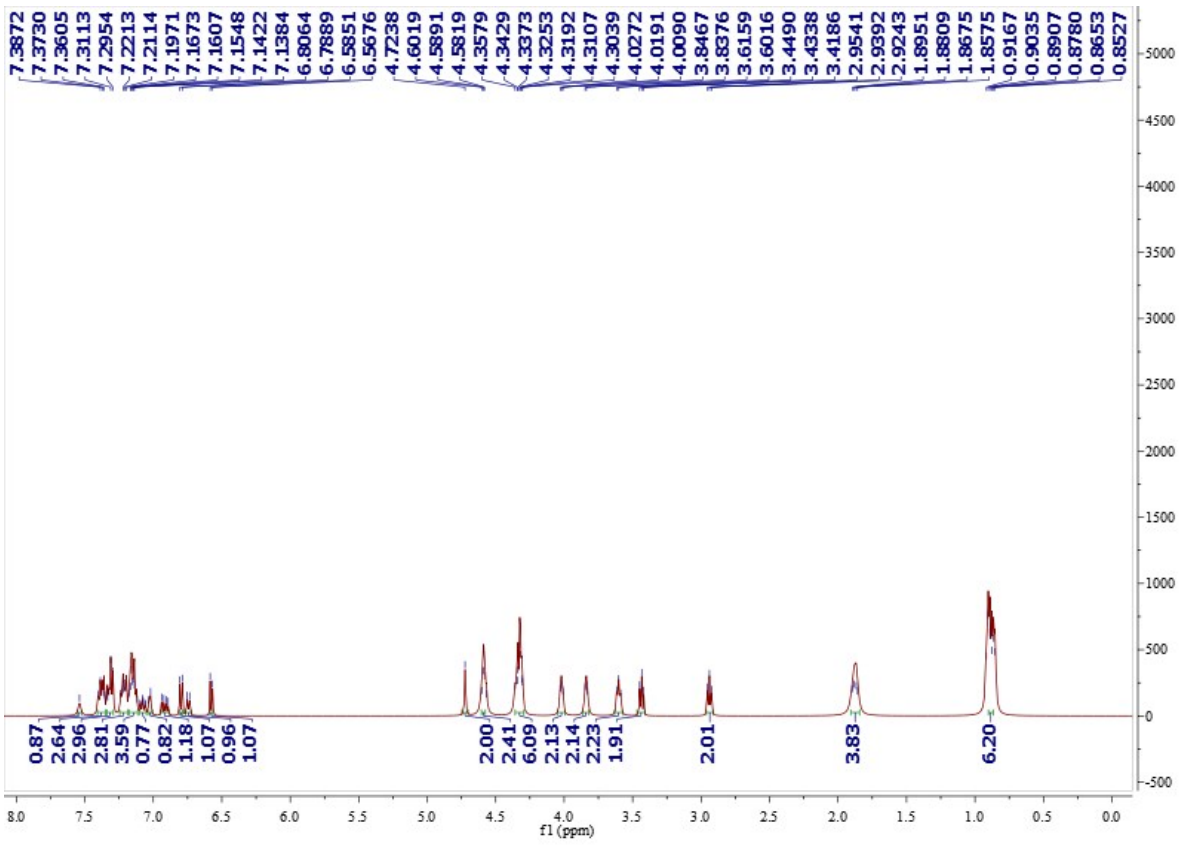

^{13}C NMR of (Z)-5-chloro-1-(8-(4-((2-(4-(4-chloro-1,2-diphenylbut-1-en-1-yl)phenoxy)ethoxy)methyl-1*H*-1,2,3-trazol-1-yl)octyl)spiro[indoline-3,2'-[1,3]dioxolan]-2-one (12e):

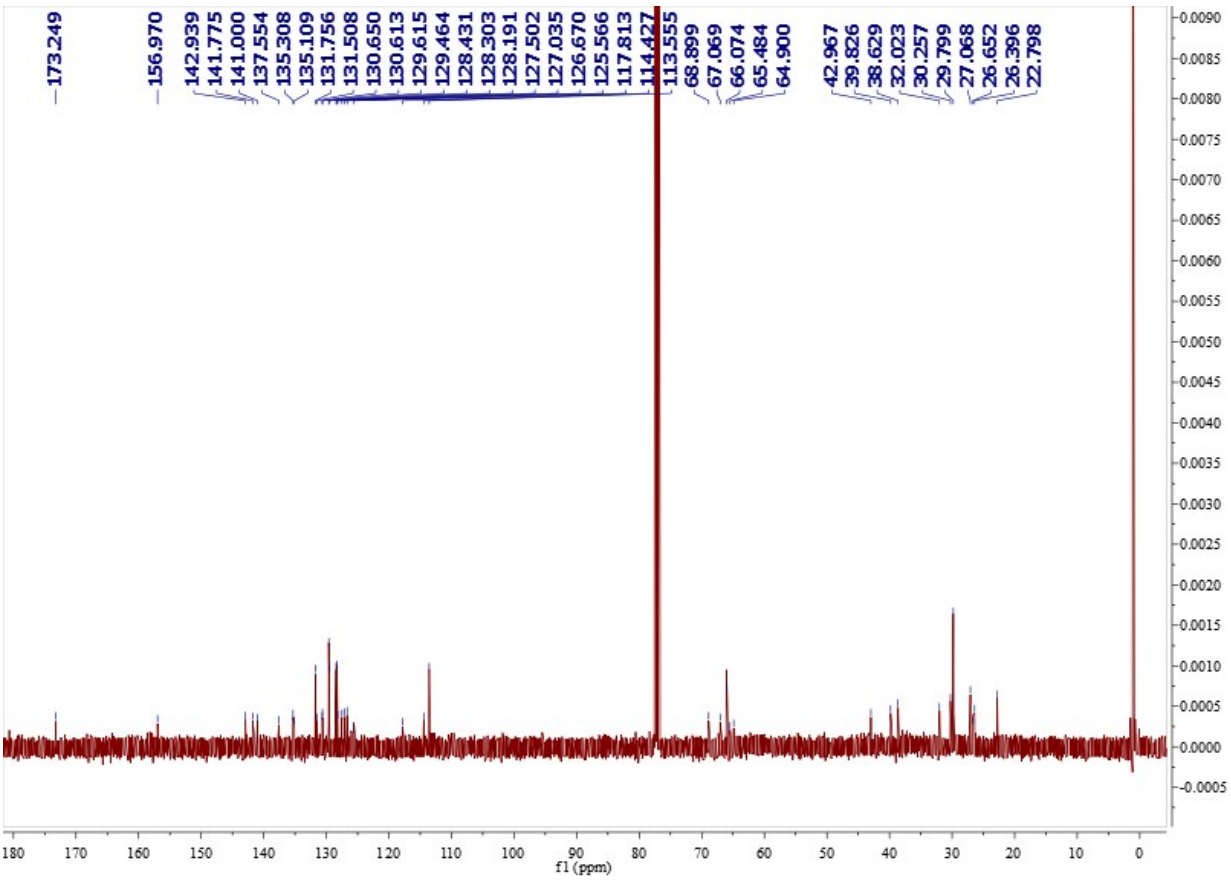

Figures:

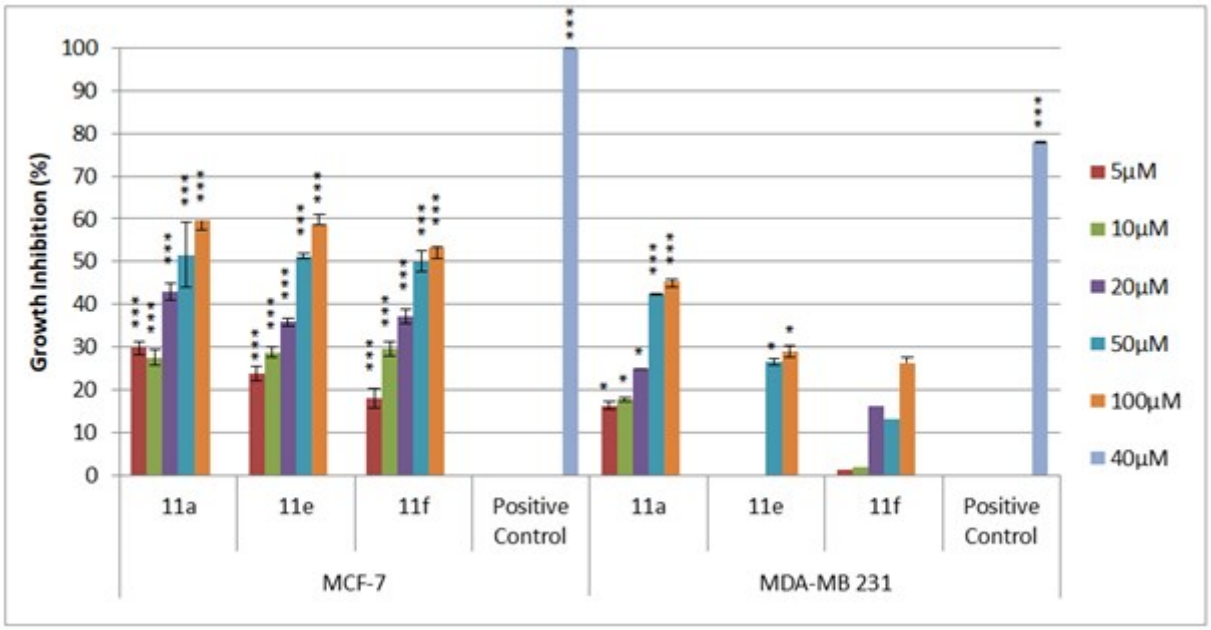

Figure 3: A representative graph comparing the percentage cell death of MCF-7 and MDA-MB-231 cells at selected concentrations of test compounds 11a, 11e and 11f. 40 µM Plumbagin was used as a positive control. Data are mean ± standard deviation (S.D.) (n=3), where *p<0.05, **p<0.01 and ***p<0.001 significant difference to untreated control.

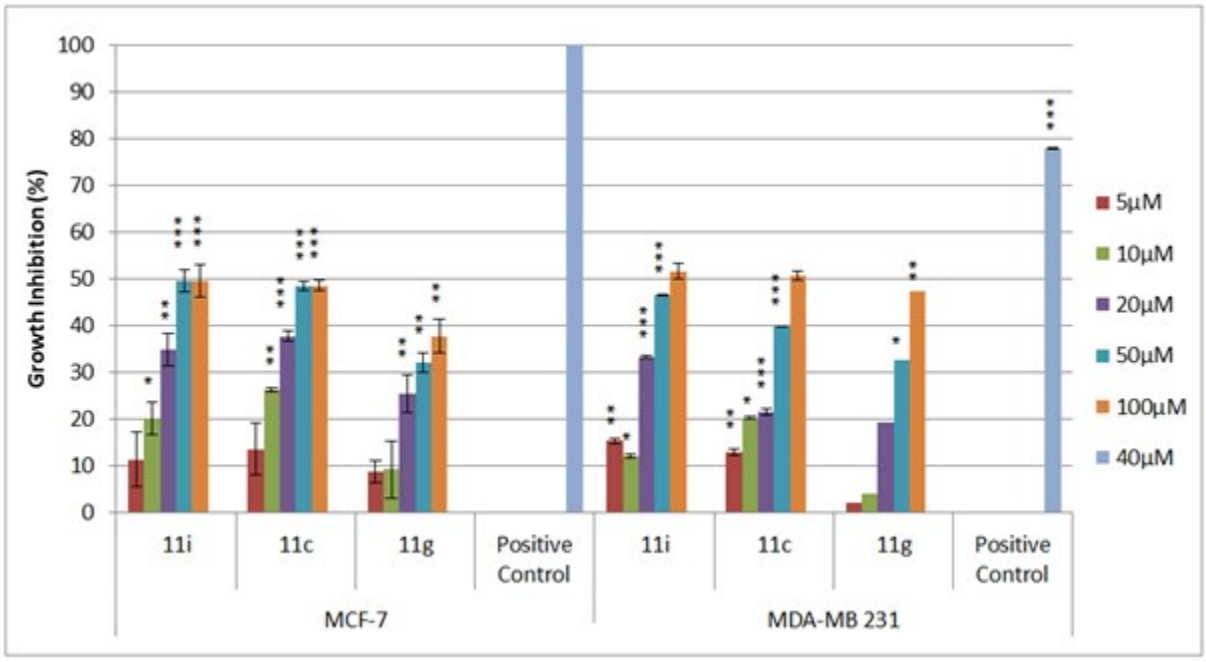

Figure 4: Representative graph comparing the percentage cell death of MCF-7 and MDA-MB-231 cells at selected concentrations of test compounds 11i, 11c and 11g.40 µM Plumbagin was used as a positive control. Data are mean ± S.D. (n=3), where *p<0.05,**p<0.01 and ***p<0.001 significant difference to untreated control.

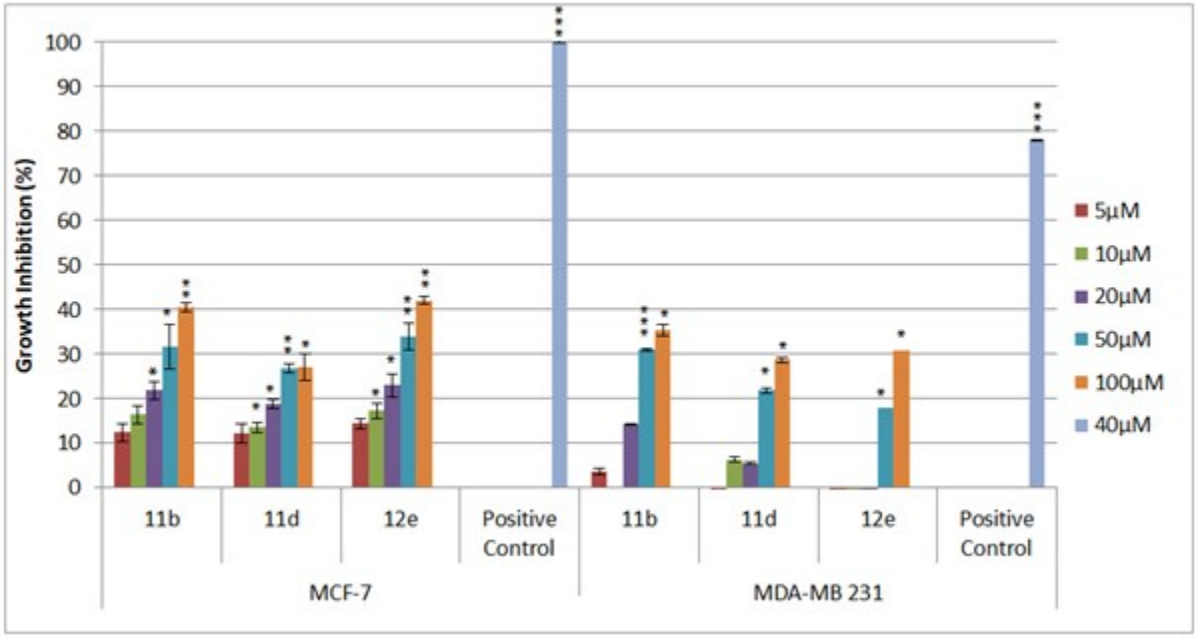

Figure 5: Representative graph comparing the percentage cell death of MCF-7 and MDA-MB-231 cells at selected concentrations of test compounds 11b, 11d and 12e. 40 µM Plumbagin was used as a positive control.Data are mean ± S.D. (n=3), where *p<0.05, **p<0.01 and ***p<0.001 significant difference to untreated control.

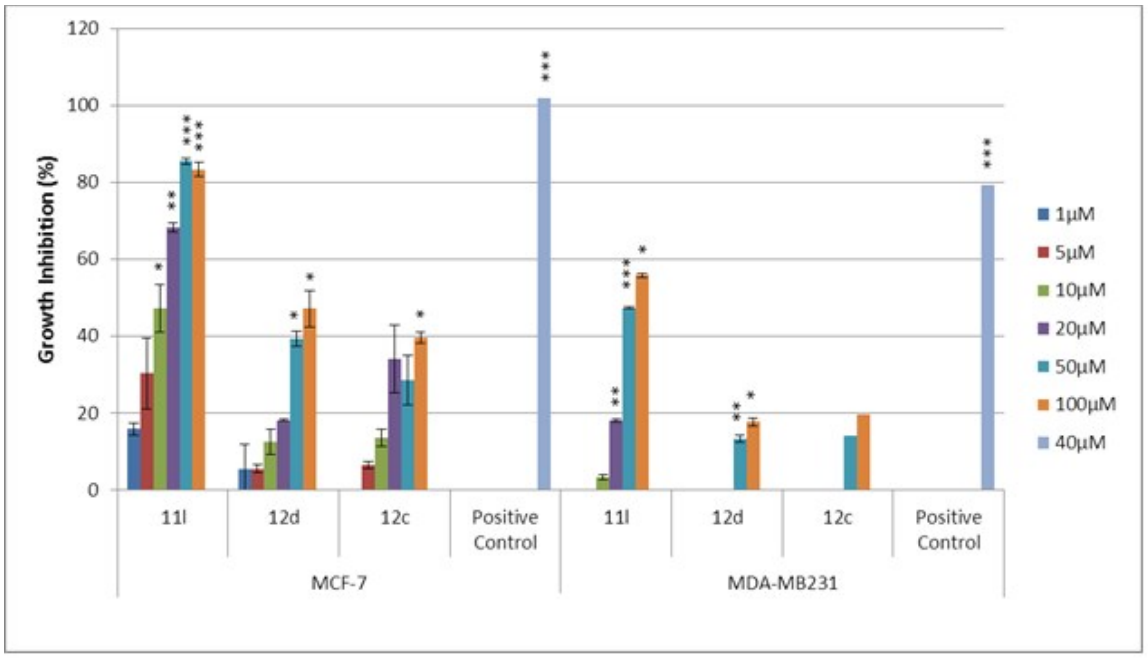

Figure 6: Representative graph comparing the percentage cell death of MCF-7 and MDA-MB-231 cells at selected concentrations of test compounds 11l, 12d and 12c. 40 μM Plumbagin was used as a positive control. Data are mean ± S.D. (n=3), where *p<0.05, **p<0.01 and ***p<0.001 significant difference to untreated control.

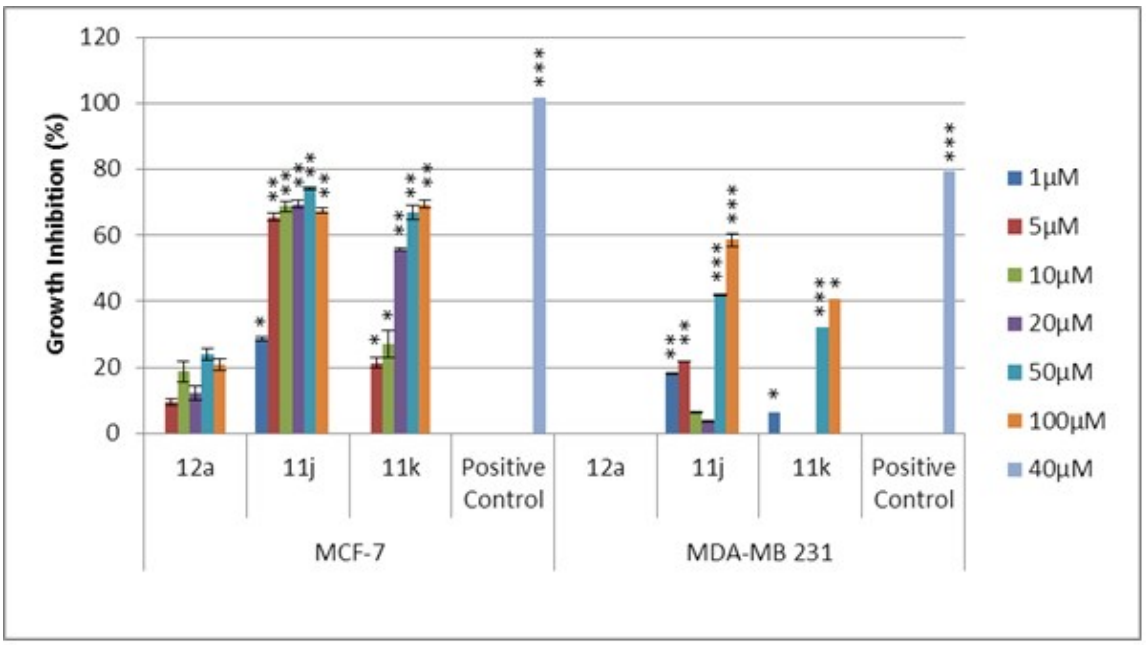

Figure 7: Representative graph comparing the percentage cell death of MCF-7 and MDA-MB-231 cells at selected concentrations of test compounds 12a, 11j and 11k. 40 μM Plumbagin was used as a positive control. Data are mean ± S.D. (n=3), where *p<0.05, **p<0.01 and ***p<0.001 significant difference to untreated control.

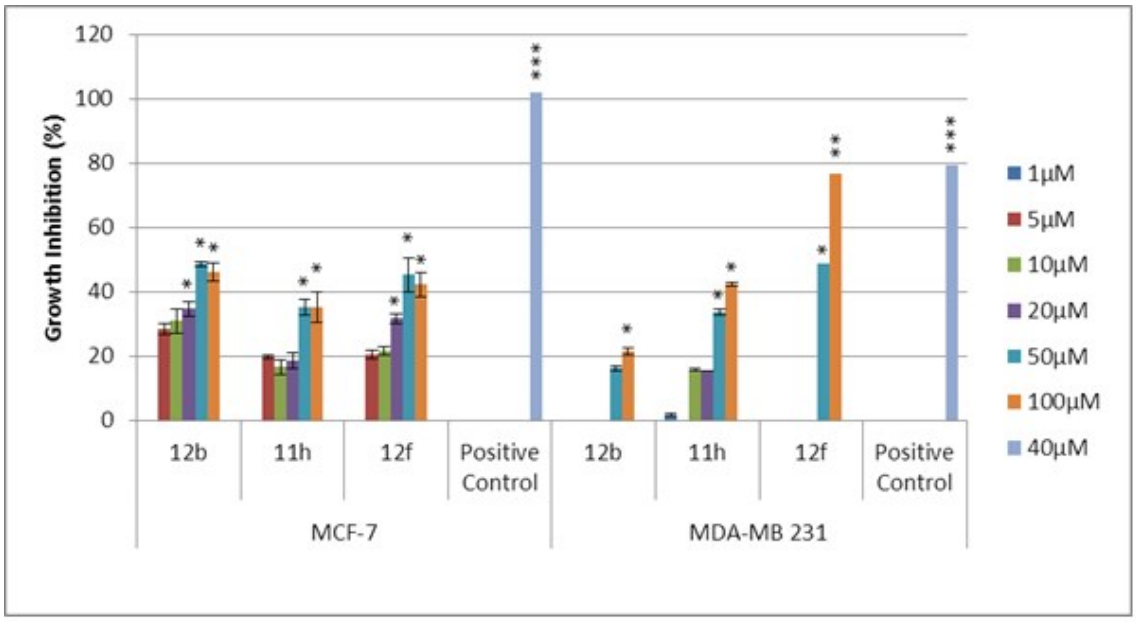

Figure 8: Representative graph comparing the percentage cell death of MCF-7 and MDA-MB-231 cells at selected concentrations of test compounds 12b, 11h and 12f. 40 µM Plumbagin was used as a positive control. Data are mean ± S.D. (n=3), where *p<0.05, **p<0.01 and ***p<0.001 significant difference to untreated control.

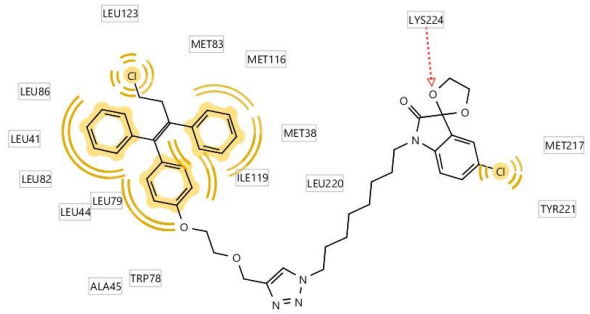

12e

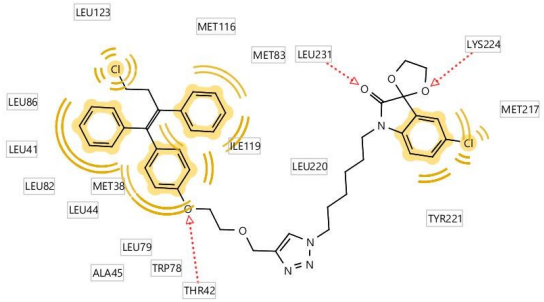

11d

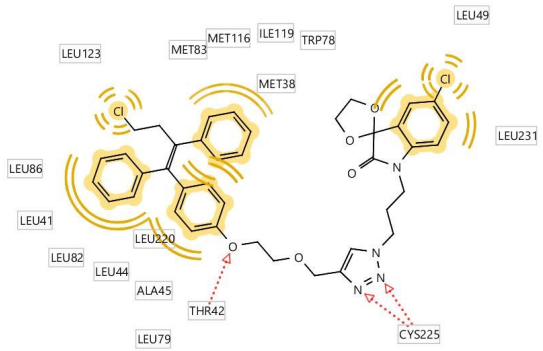

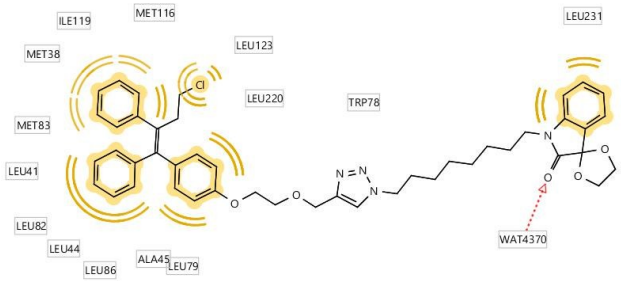

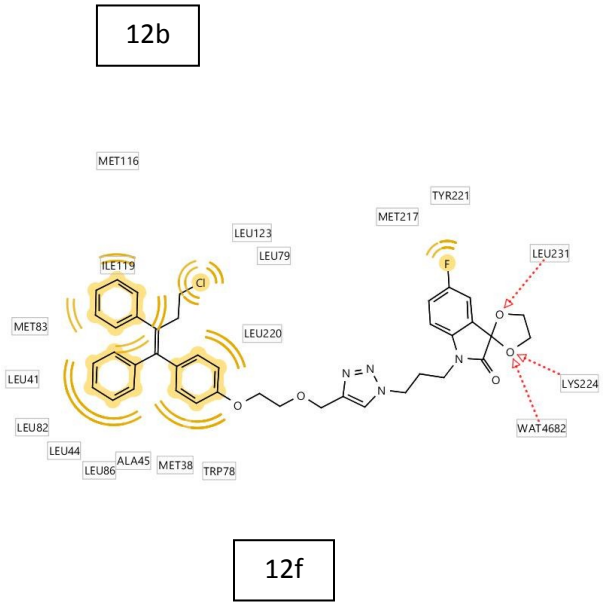

Figure 9: Ligand-protein interaction profile of ERα complexes of the least active compounds 11c, 11d, 12b, 12e, 12f.

Tables:

Table 2: Docking score of the test ligands and positive controls

Ligand identifier	Docking score/ (kcal/mol)	RMSD l.b.*	RMSD u.b.*
Ospemifene	-9.1	0.000	0.000
Plumbagin	-6.9	0.000	0.000
Tamoxifen	-9.5	0.000	0.000
11a	-10.4	1.454	1.938
11f	-9.9	1.802	2.525
11e	-10.5	0.000	0.000
11g	-10.5	2.166	3.252
11i	-10.4	0.000	0.000
11c	-10.2	0.000	0.000

11b	-10.1	1.775	3.902
11d	-9.6	0.000	0.000
12e	-9.6	1.533	2.514
12a	-10.2	2.122	3.551
*11j	-10.7	0.000	0.000
11k	-10.5	0.000	0.000
11l	-10.3	0.000	0.000
12d	-10.0	2.566	5.156
12c	-10.8	0.000	0.000
12b	-9.8	0.000	0.000
11h	-9.4	1.933	3.905
12f	-10.2	2.564	3.814

* RMSD l.b- root mean square deviation of lower bound conformation; RMSD u.b.- root mean square deviation of upper bound conformation (The two variants of RMSD measure the differences in atom conformation ignoring symmetry)

Table 3: Flexibility and Polarity features estimated using Ligand Scout

Ligand identifier	TPSA	clogP	Rotatable bonds	Aromatic atoms
11j	86.550	6.175	14	29
11k	86.550	8.084	15	29
11l	86.550	8.475	16	29
12e	87.940	8.845	20	29
12d	87.940	8.059	18	29
12c	87.940	6.889	15	29
12b	87.940	8.186	20	29
12f	87.940	6.374	15	29
Ospemifene	29.460	5.640	9	18

Table 4: Grid point parameters for docking

Grid Point Parameters	
Grid center co-ordinates	**Grid size**
X = 30.173	X = 40

Y = -1.997 Z = 24.207	Y = 30 Z = 40